

Protein Kinase C α Activates c-Src and Induces Podosome Formation via AFAP-110

Amanda Gatesman,¹ Valerie G. Walker,¹ Joseph M. Baisden,¹ Scott A. Weed,²
and Daniel C. Flynn^{1*}

The Mary Babb Randolph Cancer Center and Department of Microbiology, Immunology, and Cell Biology, West Virginia University, Morgantown, West Virginia,¹ and Department of Craniofacial Biology, University of Colorado Health Sciences Center, Denver, Colorado²

Received 15 January 2004/Returned for modification 27 February 2004/Accepted 14 May 2004

We report that the actin filament-associated protein AFAP-110 is required to mediate protein kinase C α (PKC α) activation of the nonreceptor tyrosine kinase c-Src and the subsequent formation of podosomes. Immunofluorescence analysis demonstrated that activation of PKC α by phorbol 12-myristate 13-acetate (PMA), or ectopic expression of constitutively activated PKC α , directs AFAP-110 to colocalize with and bind to the c-Src SH3 domain, resulting in activation of the tyrosine kinase. Activation of c-Src then directs the formation of podosomes, which contain cortactin, AFAP-110, actin, and c-Src. In a cell line (CaOV3) that has very little or no detectable AFAP-110, PMA treatment was unable to activate c-Src or effect podosome formation. Ectopic expression of AFAP-110 in CaOV3 cells rescued PKC α -mediated activation of c-Src and elevated tyrosine phosphorylation levels and subsequent formation of podosomes. Neither expression of activated PKC α nor treatment with PMA was able to induce these changes in CaOV3 cells expressing mutant forms of AFAP-110 that are unable to bind to, or colocalize with, c-Src. We hypothesize that one major function of AFAP-110 is to relay signals from PKC α that direct the activation of c-Src and the formation of podosomes.

Activation of either protein kinase C α (PKC α) or c-Src results in similar effects on cell morphology, including changes in actin filament integrity, cell shape changes, and stimulation of signals associated with increased motility and invasion (20, 21, 23). Several studies support the existence of cross talk between c-Src- and PKC α -mediated signaling pathways. Constitutive activation of c-Src or stable expression of v-Src will concomitantly stimulate an increase in PKC α signaling (8, 37, 44). These data indicate that PKC α could function downstream of c-Src. However, other data support a hypothesis that PKC α can signal upstream of c-Src and stimulate c-Src activity. Activation of PKC α has been demonstrated to initiate changes in actin filaments that resemble those that occur in Src^{527F}-transformed cells (7, 9, 11, 16). Likewise, it was demonstrated that stimulation of cells with phorbol esters will direct activation of c-Src in SH-SY5Y cells (5), while treatment of mouse epidermis with the tumor promoter tetradecanoyl phorbol acetate induced dose-dependent increases in c-Src kinase activity and the phosphotyrosine content of the ErbB2 receptor, which correlated with tumor-promoting ability (43). Furthermore, it was demonstrated that PKC α can directly stimulate c-Src activity in A7r5 rat aortic smooth muscle cells, and the induction of Src kinase activity is necessary for PKC-mediated actin reorganization (3). Thus, these data indicate that PKC α may function upstream as an activator of c-Src. Although PKC α is able to phosphorylate c-Src (15, 31), *in vitro* studies indicate that PKC α does not activate c-Src directly (4, 29). Thus, although these reports demonstrate the ability of PKC α to direct

activation of c-Src, the mechanism of PKC α -mediated c-Src activation is unclear.

AFAP-110 is an adaptor protein that has been demonstrated to bind to Src via SH2 and SH3 interactions (17, 18) and that will bind to PKC α via the amino-terminal pleckstrin homology (PH1) domain (32). A carboxy-terminal leucine zipper (Lzip) motif stabilizes AFAP-110 multimer formation and provides an autoinhibitory regulatory function for AFAP-110 (1, 32, 33, 35). While expression of wild-type AFAP-110 has little effect on cell morphology, deletion of the Lzip motif (AFAP-110 ^{Δ Lzip}) followed by ectopic expression of AFAP-110 ^{Δ Lzip} results in significant changes in cell morphology, including loss of actin filament organization and podosome formation, a feature common to Src-transformed cells (10, 26, 28, 30, 32–34, 39). The ability of AFAP-110 ^{Δ Lzip} to alter actin filament integrity was attributed to an ability to activate c-Src via SH3 binding, a function wild-type AFAP-110 was unable to accomplish (1). Point mutations that abolished the ability of AFAP-110 to bind to the Src SH3 domain (Pro⁷¹→Ala) also prevented AFAP-110^{71A/ Δ Lzip} from activating c-Src (1, 17). Thus, AFAP-110 has an intrinsic ability to activate c-Src as an SH3 binding partner, and this function is regulated by the Lzip motif.

Changes in the conformation of AFAP-110 and its ability to multimerize via the Lzip motif occur in transformed cells, indicating that specific cellular signals may direct AFAP-110 to activate c-Src by relieving the autoinhibitory function of the Lzip motif. Recent work in our laboratory indicated that PKC α may be positioned to fulfill this function (32). The stability of the AFAP-110 multimer is hypothesized to be governed by interactions between the Lzip motif and the amino-terminal PH1 domain (35). PKC α will bind to the PH1 domain, and these sequences overlap with sequences that bind to the Lzip motif (32, 35). Thus, PKC α binding and subsequent phosphor-

* Corresponding author. Mailing address: The Mary Babb Randolph Cancer Center and Department of Microbiology, Immunology, and Cell Biology, West Virginia University, Morgantown, WV 26506-9300. Phone: (304) 293-6966. Fax: (304) 293-4667. E-mail: dfflynn@hsc.wvu.edu.

ylation could displace the Lzip motif from intra- or intermolecular interactions and effect a conformational change that relieves the autoinhibitory function of the Lzip motif. Therefore, we hypothesized that the deletion of the Lzip motif of AFAP-110 mimicked the conformation and activity of PKC α -phosphorylated AFAP-110 and resulted in a dominant-positive form of AFAP-110 capable of independently activating c-Src.

These data led us to hypothesize that PKC α may induce the activation of c-Src in an AFAP-110-dependent fashion. We predicted that PKC α would be able to direct a conformational change in AFAP-110 similar to the effects of deleting the Lzip motif, which would enable AFAP-110 to direct the activation of c-Src. One major characteristic of c-Src activation is the formation of podosomes, actin-rich structures $\sim 0.5 \mu\text{m}$ in diameter that exist on the cytoplasmic face of the ventral membrane and facilitate the invasive potential of a cell (reviewed in reference 26). In Src-transformed cells, podosomes are known to contain a variety of proteins, including actin, cortactin, AFAP-110, and c-Src. In this report, we demonstrate that PKC α is able to activate c-Src and direct podosome formation in an AFAP-110-dependent fashion.

MATERIALS AND METHODS

Reagents. Dulbecco's modified Eagle's medium, rhodamine-phalloidin, TRITC-anti-mouse immunoglobulin G (IgG), TRITC-anti-rabbit IgG, anticortactin monoclonal antibody (MAb), and anti-Flag polyclonal antibodies and MAbs were purchased from Sigma. Phorbol 12-myristate 13-acetate (PMA) and bisindolylmaleimide [I] were obtained from Calbiochem. PKC isoform antibodies (PKC sampler kit) and antiphosphotyrosine MAbs and polyclonal antibodies were obtained from BD Transduction Laboratories. The AFAP-110 antibodies F1 and 4C3 were generated and characterized as previously described (36). Anti-Src (N-18) and anti-Src (N-16) polyclonal antibodies were purchased from Santa Cruz, while EC10 MAb and recombinant c-Src used in the Src kinase assay were obtained from Upstate Biotechnology. Phospho-src family (Tyr416) antibody was purchased from Cell Signaling. Cy5 anti-mouse IgG and Cy5 anti-rabbit IgG were obtained from Rockland. All Alexa Fluor antibodies used in the study were purchased from Molecular Probes.

AFAP-110 expression vectors. The pEGFP-c3 expression system from Amersham was used to express green fluorescent protein (GFP)-tagged forms of AFAP-110. AFAP-110 was cloned into this vector as previously described (34). CMV-1-AFAP-110 $\Delta 180-226$ was previously described (1). Fragments from CMV-AFAP-110, CMV-1-AFAP-110 $\Delta 180-226$, and GEX-6P-AFAP-110 71A were subcloned into pEGFP-c3-AFAP-110 to create full-length, GFP-tagged forms of these mutants. CMV-AFAP-110 $^{71A/\Delta Lzip}$ and CMV-AFAP-110 $\Delta 180-226/\Delta Lzip$ were generated as previously described (1). Flag-myr-PKC α and Flag-d/nPKC α were kind gifts from A. Tokar.

Src kinase assay. The abilities of recombinant wild-type AFAP-110 (rAFAP-110) and rAFAP-110 $\Delta Lzip$ to activate c-Src were assessed by using a modified Src kinase assay protocol from Upstate Biotechnology. Briefly, GST-AFAP-110, GST-AFAP-110 $\Delta Lzip$, and GST-Csk were immobilized on glutathione-Sepharose 4B beads from Amersham as previously described (17). Recombinant c-Src (Upstate Biotechnology) was inactivated by incubation with GST-Csk in Csk buffer (10 mM HEPES, pH 7.4, 5 mM MnCl $_2$, 100 μM ATP) for 30 min at 30°C. The GST-Csk was removed by centrifugation, and the inactive c-Src was aliquoted into 1.5-ml tubes. The GST-AFAP-110 and GST-AFAP-110 $\Delta Lzip$ were washed in mouse tonicity-phosphate-buffered saline with 1% Triton-X and then in Src kinase buffer (100 mM Tris-HCl, 125 mM MgCl $_2$, 25 mM MnCl $_2$, 2 mM EGTA, pH 8.0, 250 μM NaO $_3$, 2 mM dithiothreitol). The Src kinase reaction was carried out for 1 min in the presence of Mg-ATP. The reactions were stopped by the addition of 0.5 M EGTA, and the samples were separated by sodium dodecyl sulfate-8% polyacrylamide gel electrophoresis (SDS-8% PAGE) and transferred to polyvinylidene difluoride membranes. The membranes were probed with antiphosphotyrosine antibody to demonstrate AFAP-110 phosphorylation.

Cell culture and immunofluorescence. SYF, SYF/c-Src, and CaOV3 cells were cultured in Dulbecco's modified Eagle's medium supplemented with 10% fetal calf serum. Transient transfection of SYF, SYF/c-Src, and CaOV3 cells for

immunofluorescence was carried out using Lipofectamine reagent (Invitrogen) according to the manufacturer's protocol. Thirty-six hours after transfection, SYF and SYF/c-Src cells were serum starved for 12 h, while CaOV3 cells were serum starved for 18 h, and all of the cells were subsequently fixed and permeabilized as previously described (33). For actin labeling, a 1:1,000 dilution of tetramethyl rhodamine isothiocyanate (TRITC)-phalloidin was used. The antibody concentrations used were as follows: F1, 1:200 in 5% milk-TBS-T; anti-Flag MAb, 1:1,000 in 5% bovine serum albumin (BSA); anti-Flag polyclonal antibody, 1:200 in 5% BSA; EC10, 1:500 in 5% BSA; antiphosphotyrosine polyclonal antibody, 1:100 in 5% BSA; antiphosphotyrosine MAb, 1:200 in 5% BSA; phospho-Src family (Y416), 1:250 in 5% BSA; anti-Src (N18), 1:500 in 5% milk-TBS-T; anticortactin polyclonal antibody, 1:1,000 in 5% BSA; anticortactin MAb, 1:500 in 5% BSA. All fluorescent secondary antibodies were diluted 1:200 in 5% BSA and are labeled according to use in the figure legends. Cells were washed and mounted on slides with Fluoromount-G (Fisher). A Zeiss LSM 510 microscope was used to gather images, which represent confocal slices $\sim 1 \mu\text{M}$ thick. To prevent cross-contamination among the different fluorochromes, each channel was imaged sequentially using the multitrack recording module before the images were merged. Scale bars were generated and inserted by LSM 510 software. For all figures, representative cells are shown (>100 cells were examined per image shown).

RESULTS

PKC α requires the presence of c-Src to effect changes in actin filament integrity and podosome formation. It was previously demonstrated that PKC α can direct the activation of c-Src in A7r5 rat aortic smooth muscle cells in response to phorbol ester treatment (3). We sought to verify this finding in our cell system using SYF cells, which are derived from mouse embryonic fibroblasts engineered to contain null mutations in the *c-src*, *fyn*, and *c-yes* genes (24) and which therefore do not express Src family tyrosine kinases. We also utilized SYF/c-Src cells, which are derived from SYF cells and express only the c-Src tyrosine kinase family member, to examine the effects of expressing a constitutively active form of PKC α (myrPKC α) upon c-Src activation and changes in actin filament organization. Expression of myrPKC α in SYF/c-Src cells resulted in altered actin stress filament integrity, with actin filaments reorganized into actin-rich, podosome-like structures (Fig. 1A, images b and f). These actin-rich structures were between 0.2 and 0.5 μm in diameter and were apparent on the cytoplasmic face of the ventral membrane, consistent with the definition of a podosome (26). There was also an increase in cellular tyrosine phosphorylation (Fig. 1A, image c), as well as activation of c-Src (Fig. 1A, image g). To confirm that these actin-rich, podosome-like structures generated in response to myrPKC α were actually podosomes, SYF/c-Src cells expressing myrPKC α were labeled for cortactin, a protein known to be present in podosomes subsequent to c-Src activation (Fig. 1B, image k) (reviewed in reference 26). The data demonstrate that cortactin colocalizes with actin in these structures, confirming their identities as podosomes (Fig. 1B, image l). Finally, expression of a dominant-negative form of PKC α (Fig. 1, image m) was unable to effect actin-rich podosome formation or direct an increase in cellular tyrosine phosphorylation (Fig. 1B, images m to p). These results confirm that c-Src is activated in response to PKC α activity, and this correlates with elevated levels of cellular tyrosine phosphorylation and changes in actin filament integrity, including the formation of podosomes.

In order to determine if PKC α requires the presence of c-Src to effect changes in actin filament integrity, c-Src and myrPKC α were expressed together or separately in SYF cells in the presence of GFP epitope-tagged AFAP-110, which has

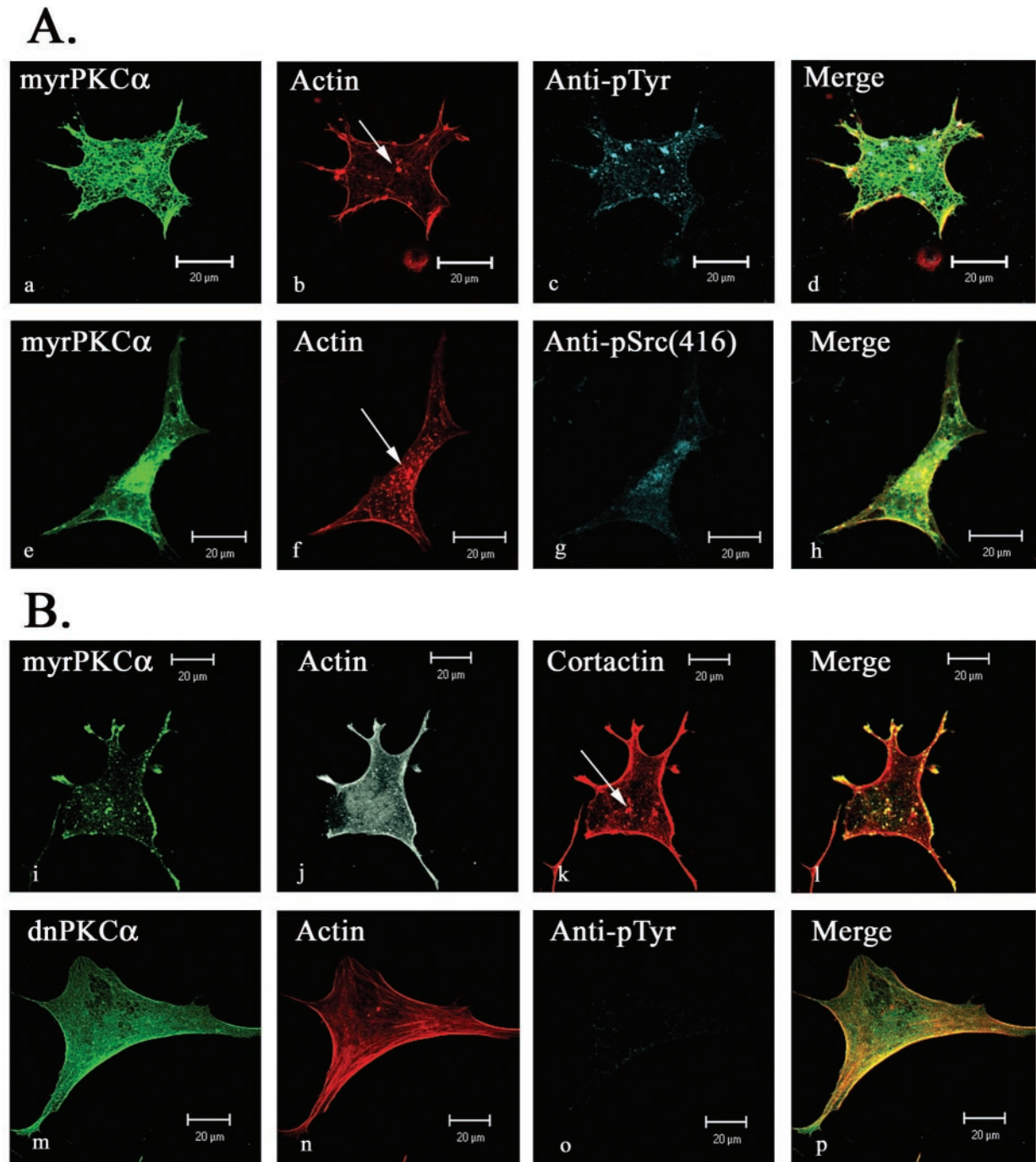


FIG. 1. Myristoylated PKC activates c-Src and alters actin filaments. (A) SYF/c-Src cells were transiently transfected with Flag-tagged myristoylated PKC and labeled with anti-Flag antibody (a and e), antiphosphotyrosine (c), phospho-Src family (Y416) antibody (g), and TRITC-phalloidin (b and f). Expression of myrPKC resulted in the loss of actin filament integrity and the formation of actin-rich podosome-like structures (b and f, arrows). These cells also displayed an increase in c-Src phosphorylation at the Y416 position (g). (B) SYF/c-Src cells were transiently transfected with Flag-tagged myristoylated PKC or Flag-tagged dominant-negative PKC and labeled with anti-Flag antibody (i and m), anticortactin (k), antiphosphotyrosine (o), and TRITC-phalloidin (j and n). Expression of myrPKC resulted in the formation of actin-rich podosomes along the ventral surface, as indicated by the presence of cortactin in these structures (j and k, arrows). Likewise, actin and cortactin are observed to colocalize in the merged image (l). Expression of dominant-negative PKC (m) resulted in no changes in actin filament integrity (n) or immunoreactivity with the antiphosphotyrosine antibody (o). Anti-Flag MAb was visualized with Alexa Fluor 488–goat anti-mouse IgG. Antiphosphotyrosine and phospho-Src family (Y416) antibody were visualized with Alexa Fluor 647–goat anti-rabbit IgG. Anticortactin was visualized with Alexa Fluor 647–goat anti-mouse IgG.

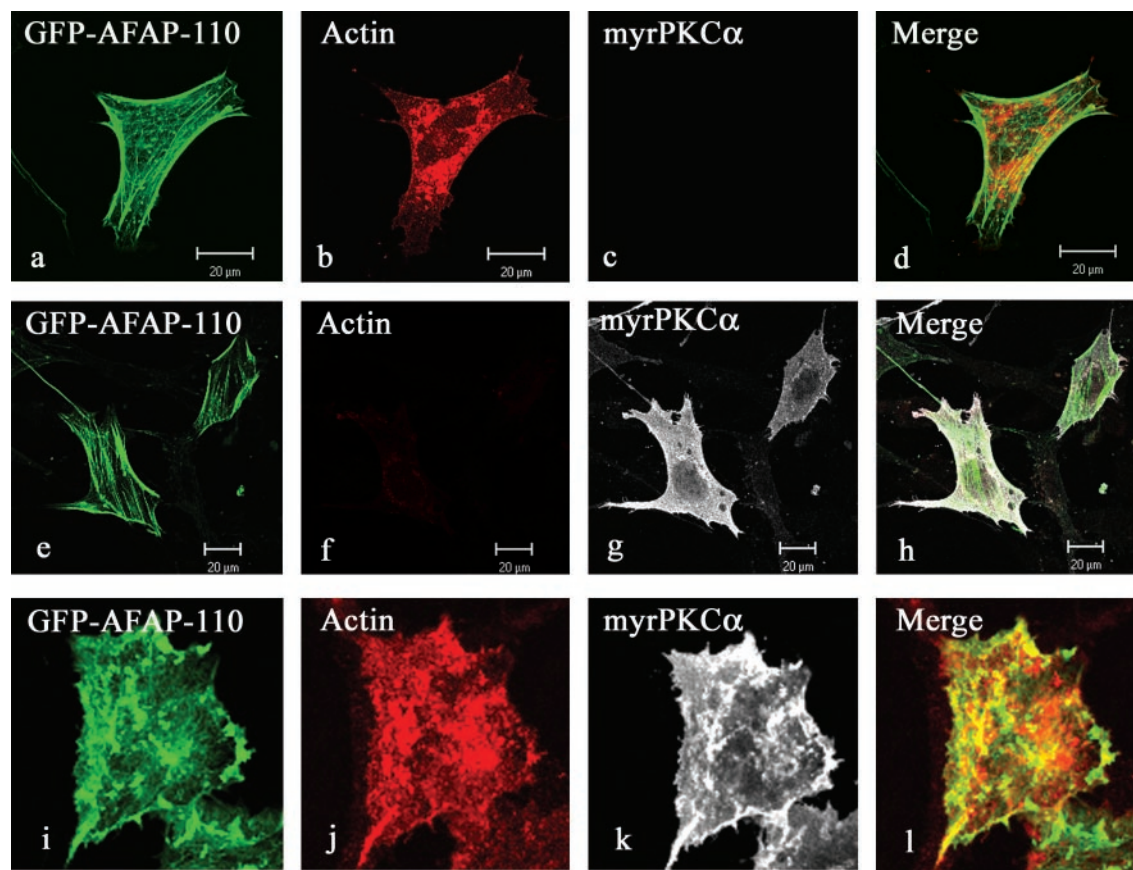
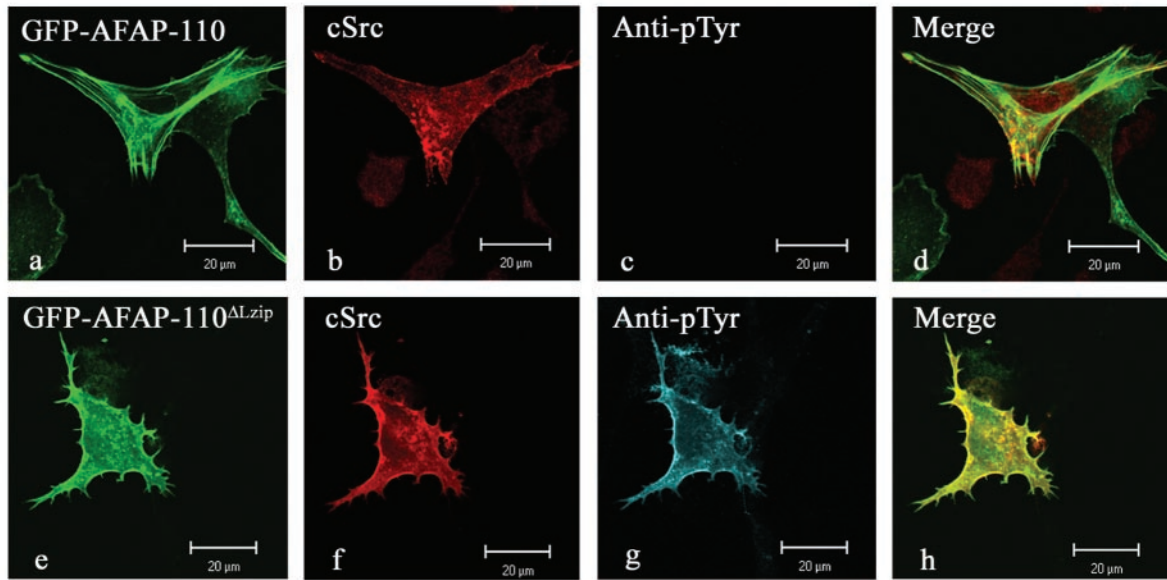


FIG. 2. Myristoylated PKC alters actin filament integrity in a c-Src-dependent fashion in SYF cells. (Top row) SYF cells were transiently transfected with both GFP-AFAP-110 (a) and pCMV-c-Src and immunolabeled with EC10 antibody (b). (a to d) In the absence of myrPKC, SYF cells have normal morphology and numerous actin stress fibers. (d) Also, c-Src and GFP-AFAP-110 do not appear to colocalize. (Middle row) SYF cells were transiently transfected with both GFP-AFAP-110 (e) and Flag-tagged myrPKC and immunolabeled with anti-Flag antibody (g). (e to h) In the absence of c-Src, SYF cells display well-formed actin filaments and have normal morphology. (Bottom row) SYF cells were transiently transfected with GFP-AFAP-110 (i), c-Src (j) and Flag-tagged myrPKC (k) and immunolabeled with MAb EC10 and anti-Flag antibody. (i to k) In the presence of both c-Src and myrPKC, SYF cells lose actin filament integrity and instead form actin-rich punctate structures (l). Furthermore, GFP-AFAP-110 and c-Src are also observed to colocalize in the presence of myrPKC (l). EC10 was visualized with Cy5 anti-mouse IgG, while anti-Flag polyclonal antibody was visualized with TRITC-anti-rabbit IgG.

been shown to colocalize with actin filaments (34). In SYF cells expressing GFP-AFAP-110 and c-Src (Fig. 2a to d), GFP-AFAP-110 highlights the cortical actin matrix and stress filaments that span the length of the cell (Fig. 2a), while c-Src exhibits a perinuclear staining pattern (Fig. 2b), consistent with previous reports that inactive c-Src is located on perinuclear vesicles (38). In the absence of c-Src, myrPKC α was unable to effect changes in AFAP-110 localization (Fig. 2e to h), and GFP-AFAP-110 localized to well-formed stress filaments and cortical actin filaments. The presence of well-formed actin filaments in these cells may be facilitated by an increased ability of AFAP-110 to cross-link actin filaments upon phosphorylation by PKC α , as noted previously (32). However, co-expression of GFP-AFAP-110 and myrPKC α with c-Src in SYF cells resulted in a complete disruption of actin filament integrity and the formation of actin-rich punctate structures, as well as the formation of motility structures, a phenotype that is a hallmark of c-Src transformation (Fig. 2i to l). These data indicate that myrPKC α requires c-Src in order to effect major changes in cell shape and the actin cytoskeleton.

AFAP-110 activates c-Src by colocalizing with and binding to the c-Src SH3 domain. Previous studies in our laboratory demonstrated that wild-type AFAP-110 is unable to stimulate the activation of c-Src in fibroblast cells, while coexpression of the dominant-positive AFAP-110^{ΔLzip} was able to direct activation of c-Src in cell culture (1, 32). The ability of AFAP-110^{ΔLzip} to activate c-Src was dependent upon SH3 interactions with the c-Src SH3 domain. Mutations that abolish SH3 binding to c-Src (Pro⁷¹→Ala⁷¹) prevent both stable complex formation with c-Src and the ability of AFAP-110^{ΔLzip/71A} to activate c-Src in cell culture (1). In order to clarify the mechanism by which AFAP-110 may be directed to activate c-Src in cell culture, we utilized confocal microscopy to analyze GFP-AFAP-110, GFP-AFAP-110^{ΔLzip}, and c-Src for colocalization and activation of cellular tyrosine phosphorylation in SYF cells (Fig. 3). Figure 3A, images a to d, demonstrates that AFAP-110 is unable to colocalize with c-Src and confirms that wild-type AFAP-110 is incapable of stimulating an increase in cellular tyrosine phosphorylation. Furthermore, there was no evidence for podosome formation based on GFP-AFAP-

A. SYF



SYF

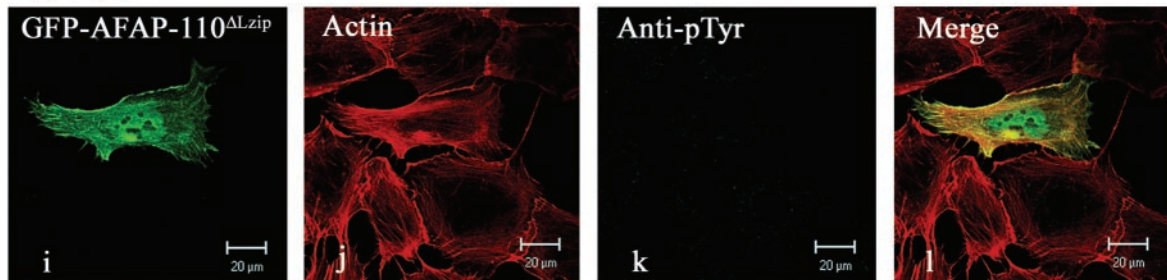
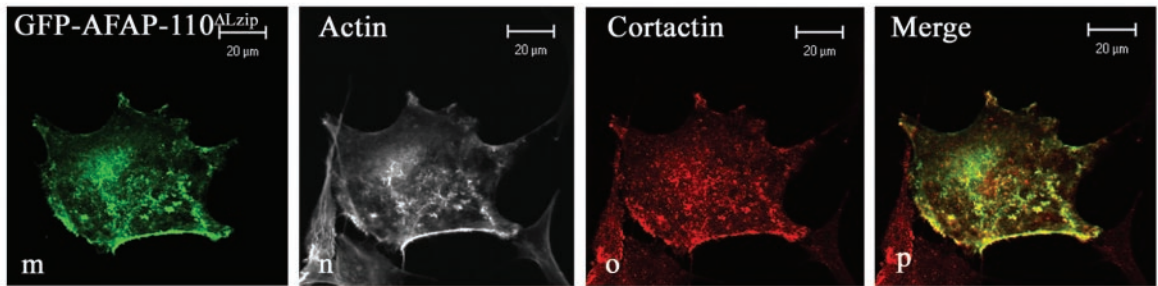


FIG. 3. Ability of dominant-positive AFAP-110 to activate c-Src correlates with colocalization of AFAP-110 with c-Src. (A) SYF cells were transiently cotransfected with c-Src and either wild-type GFP-AFAP-110 (a) or dominant-positive GFP-AFAP-110^{Lzip} (e) and immunolabeled with EC10 (b and f) and antiphosphotyrosine (c and g). Cells coexpressing GFP-AFAP-110 and c-Src display immunoreactivity with the phosphospecific antibody equivalent to that of surrounding nontransfected cells (c), as well as numerous GFP-AFAP-110-decorated actin filaments (a). Likewise, no colocalization is observed between GFP-AFAP-110 and c-Src (d). Cells coexpressing GFP-AFAP-110^{Lzip} and c-Src display increased immunoreactivity to the phosphospecific antibody (g), as well as complete disruption of actin filament integrity (e). Also, GFP-AFAP-110^{Lzip} and c-Src are observed to colocalize (h). Transfection of GFP-AFAP-110^{Lzip} alone into SYF cells (i) resulted in no alteration in actin stress fiber integrity (j), as well as no elevation in cellular tyrosine phosphorylation (k), indicating that AFAP-110^{Lzip} activates c-Src and not another tyrosine kinase present in SYF cells. (B) SYF/c-Src cells were transiently transfected with GFP-AFAP-110^{Lzip} (m) and immunolabeled with TRITC-phalloidin (n) and anticortactin (o). Expression of the Lzip mutant in SYF/c-Src cells results in a loss of actin stress fiber organization and the formation of actin-rich podosome structures (n). Cortactin is also present in these structures (o and p). (C) SYF cells were transiently cotransfected with c-Src and either GFP-AFAP-110^{71A/ΔLzip} (q) or GFP-AFAP-110^{180-226/ΔLzip} (u) and immunolabeled with EC10 (r and v) and antiphosphotyrosine (s and w). Cells coexpressing c-Src and GFP-AFAP-110^{71A/ΔLzip} display no elevation in cellular tyrosine phosphorylation (s). In the context of the dominant-positive Lzip deletion, GFP-AFAP-110^{71A/ΔLzip} and c-Src are observed to colocalize (t). Cells coexpressing c-Src and GFP-AFAP-110^{180-226/ΔLzip} display no elevation in cellular tyrosine phosphorylation immunoreactivity with the phosphospecific antibody, equivalent to surrounding nontransfected cells (w). In the context of the dominant-positive Lzip deletion, GFP-AFAP-110^{180-226/ΔLzip} and c-Src fail to colocalize (x). EC10 was visualized with Alexa Fluor 546-goat anti-mouse IgG, antiphosphotyrosine was visualized with Alexa Fluor 647-goat anti-rabbit IgG, cortactin was visualized with Alexa Fluor 647-goat anti-mouse IgG, and actin was visualized with TRITC-phalloidin.

110 localization, which decorates actin filaments. AFAP-110^{Lzip} demonstrated strong colocalization with c-Src and was able to direct the activation of cellular tyrosine phosphorylation (Fig. 3A, images e to h). GFP-AFAP-110^{Lzip} transfected into SYF cells in the absence of c-Src displayed no increased immunoreactivity to the antiphosphotyrosine antibody or evi-

dence for podosome formation (Fig. 3A, images i to l), indicating that AFAP-110^{Lzip} activates c-Src and not another tyrosine kinase present in these cells and that AFAP-110^{Lzip} requires c-Src to direct podosome formation. In the presence of c-Src, AFAP-110^{Lzip} was able to colocalize with cortactin in podosomes that were detected on the cytoplasmic face of the

B. SYF/cSrc



C. SYF

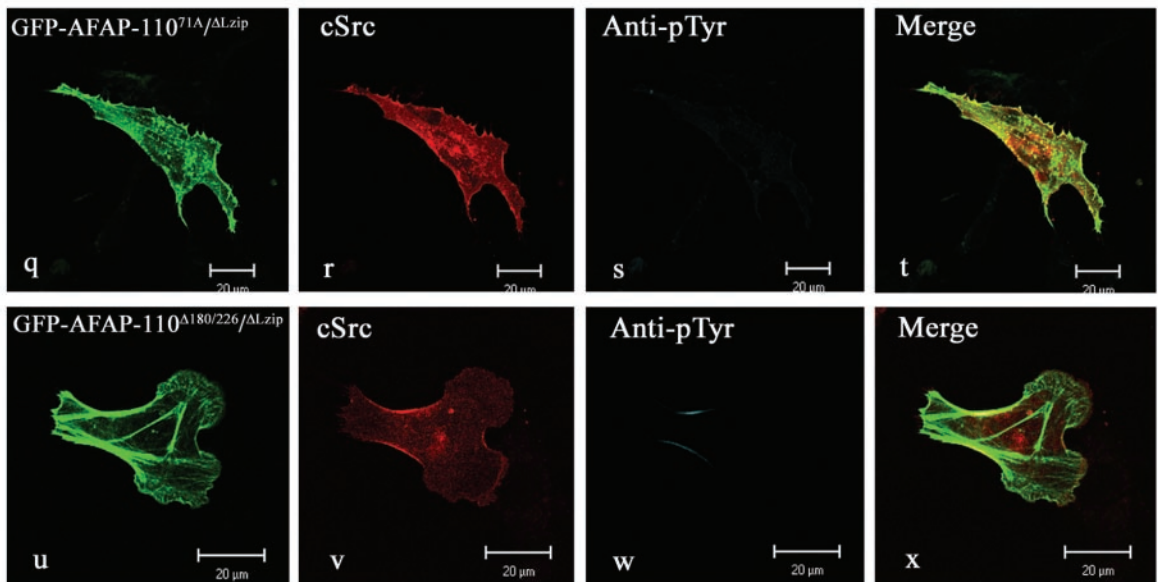


FIG. 3—Continued.

dorsal membrane of SYF/c-Src cells (Fig. 3B, images m to p). Mutants of AFAP-110 that were unable to interact with the c-Src SH3 domain (AFAP-110^{71A}) or that contained deletions in the PH1 domain and were unable to bind with PKC α (AFAP-110 Δ ¹⁸⁰⁻²²⁶) have each been shown to abolish the ability of AFAP-110 Δ Lzip to activate c-Src and alter actin filament integrity in vivo (1). AFAP-110^{71A}/ Δ Lzip was unable to direct an increase in cellular tyrosine phosphorylation, although it was able to colocalize with c-Src (Fig. 3C, images q to t). The inability to enhance cellular tyrosine phosphorylation was most likely due to its inability to engage the c-Src SH3 domain. Interestingly, AFAP-110 Δ ¹⁸⁰⁻²²⁶/ Δ Lzip was also unable to direct the elevation of cellular tyrosine phosphorylation; however, unlike AFAP-110 Δ Lzip/^{71A}, there was no evidence for colocalization with c-Src (Fig. 3C, images u to x). These cellular effects indicate that deletion of the Lzip domain derepresses an intrinsic ability of AFAP-110 to activate c-Src kinase via SH3 binding, while the integrity of the PH1 domain is required to facilitate colocalization between AFAP-110 and c-Src.

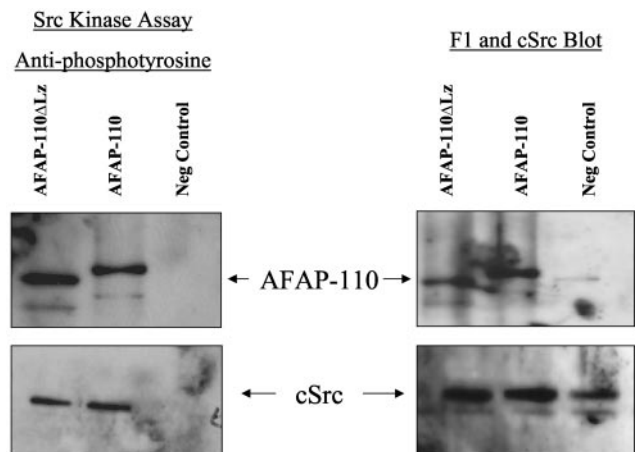


FIG. 4. Both AFAP-110 and AFAP-110 Δ Lzip are able to activate c-Src in vitro. rAFAP-110 and rAFAP-110 Δ Lzip were incubated with c-Src and subjected to an in vitro kinase assay. Western blot analysis of phosphotyrosine levels and control protein levels are shown. The blot is representative of seven separate experiments.

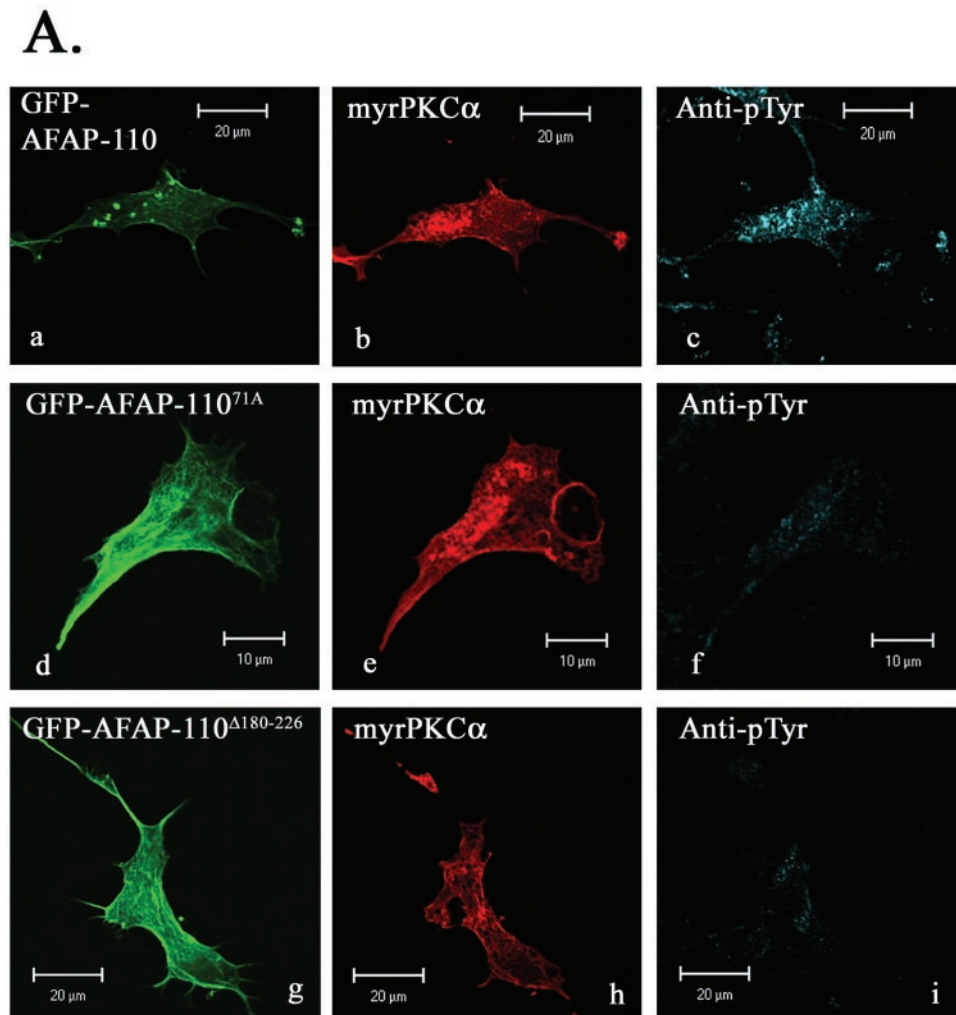


FIG. 5. PKC activates c-Src and alters actin filament integrity in an AFAP-110-dependent fashion. (A) SYF/c-Src cells were transiently cotransfected with Flag-tagged myrPKC and either GFP-AFAP-110 (a), GFP-AFAP-110^{71A} (d), or GFP-AFAP-110^{Δ180-226} (g) and labeled with anti-Flag antibody (b, e, and h) and antiphosphotyrosine (c, f, and i). Cells coexpressing GFP-AFAP-110 and myrPKC display increased immunoreactivity with the phosphotyrosine antibody compared to surrounding nontransfected cells (c). Cells coexpressing GFP-AFAP-110^{71A} and myrPKC display immunoreactivity to the phosphotyrosine antibody equivalent to that of surrounding nontransfected cells (f), as well as contiguous actin filaments coincident with AFAP-110 (d). Identical results were observed upon coexpression of GFP-AFAP-110^{Δ180-226} with myrPKC (g to i). Actin-rich punctate structure is shown. (B) SYF/c-Src cells were transiently cotransfected with Flag-tagged myrPKC and either GFP-AFAP-110 (j), GFP-AFAP-110^{71A} (m), or GFP-AFAP-110^{Δ180-226} (p) and immunolabeled with anti-Flag antibody (k, n, and q) and phospho-Src family (Y416) antibody (l, o, and r). Cells coexpressing GFP-AFAP-110 and myrPKC display increased immunoreactivity with the phospho-Src family (Y416) antibody compared to surrounding nontransfected cells (l). The arrow indicates podosomes. Cells coexpressing GFP-AFAP-110^{71A} and myrPKC display immunoreactivity to the phospho-Src family (Y416) antibody equivalent to that of surrounding nontransfected cells (o), as well as contiguous actin filaments coincident with AFAP-110 (m). Identical results were observed upon coexpression of GFP-AFAP-110^{Δ180-226} with myrPKC (p to r). Anti-Flag MAb was visualized with Alexa Fluor 647-goat anti-mouse IgG, while antiphosphotyrosine and phospho-Src family (Y416) antibodies were visualized with Alexa Fluor 546-goat anti-rabbit IgG.

It was previously hypothesized that deletion of the Lzip motif might affect a structural change that placed the SH3 binding motif in a more favorable conformation that facilitated binding to the c-Src SH3 domain and activation of c-Src (33). The data shown in Fig. 3 indicate that colocalization between AFAP-110 and c-Src may also be important. Recently, it was reported that rAFAP-110 could stimulate activation of c-Src in vitro, based on in vitro kinase assays (27). Thus, our initial hypothesis concerning how AFAP-110^{ΔLzip} could activate c-Src may not have been fully correct. To address this concern, we performed an in vitro kinase assay using rAFAP-110 or

rAFAP-110^{ΔLzip} and incubated each with recombinant c-Src that had been phosphorylated by c-Src kinase to inactivate the kinase in vitro. Measurement of tyrosine phosphorylation of rAFAP-110 or rAFAP-110^{ΔLzip} indicated that c-Src was able to become activated by, and stimulate tyrosine phosphorylation of, either rAFAP-110 or rAFAP-110^{ΔLzip} (Fig. 4). Furthermore, phosphorylation of rAFAP-110 by rPKCα did not enhance the ability of AFAP-110 to activate c-Src, relative to unphosphorylated rAFAP-110, in vitro (M. Liu, personal communication). Thus, our analysis indicates that both AFAP-110^{ΔLzip} and AFAP-110 are capable of activating c-Src activity

B.

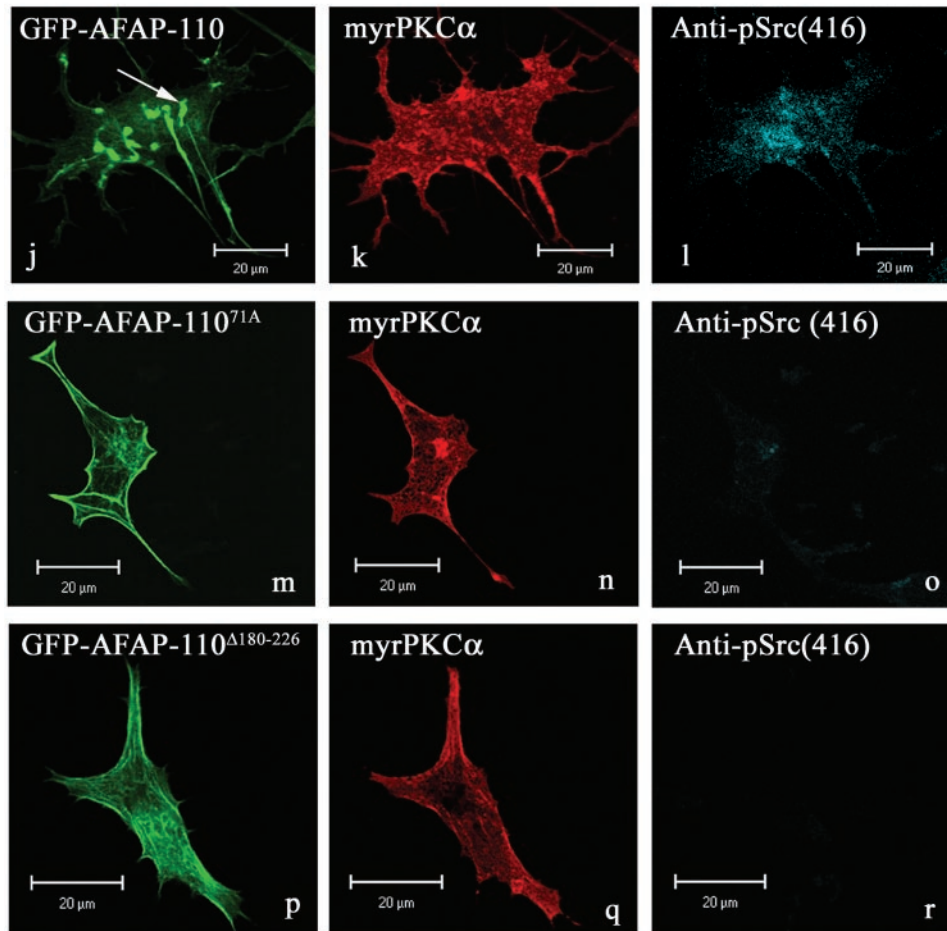


FIG. 5—Continued.

in vitro; however, only AFAP-110^{ΔLzip} activates c-Src in vivo. Thus, we predict that the ability of AFAP-110 to activate c-Src is dependent upon its ability to (i) colocalize with c-Src and (ii) bind to the c-Src SH3 domain. Therefore, deletion of the Lzip motif and release of its autoinhibitory function must allow AFAP-110 to colocalize with c-Src by an unknown mechanism, and it is this event that enables it to bind to and activate c-Src.

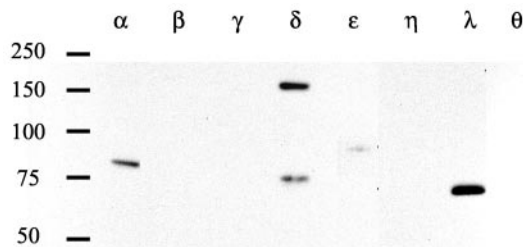
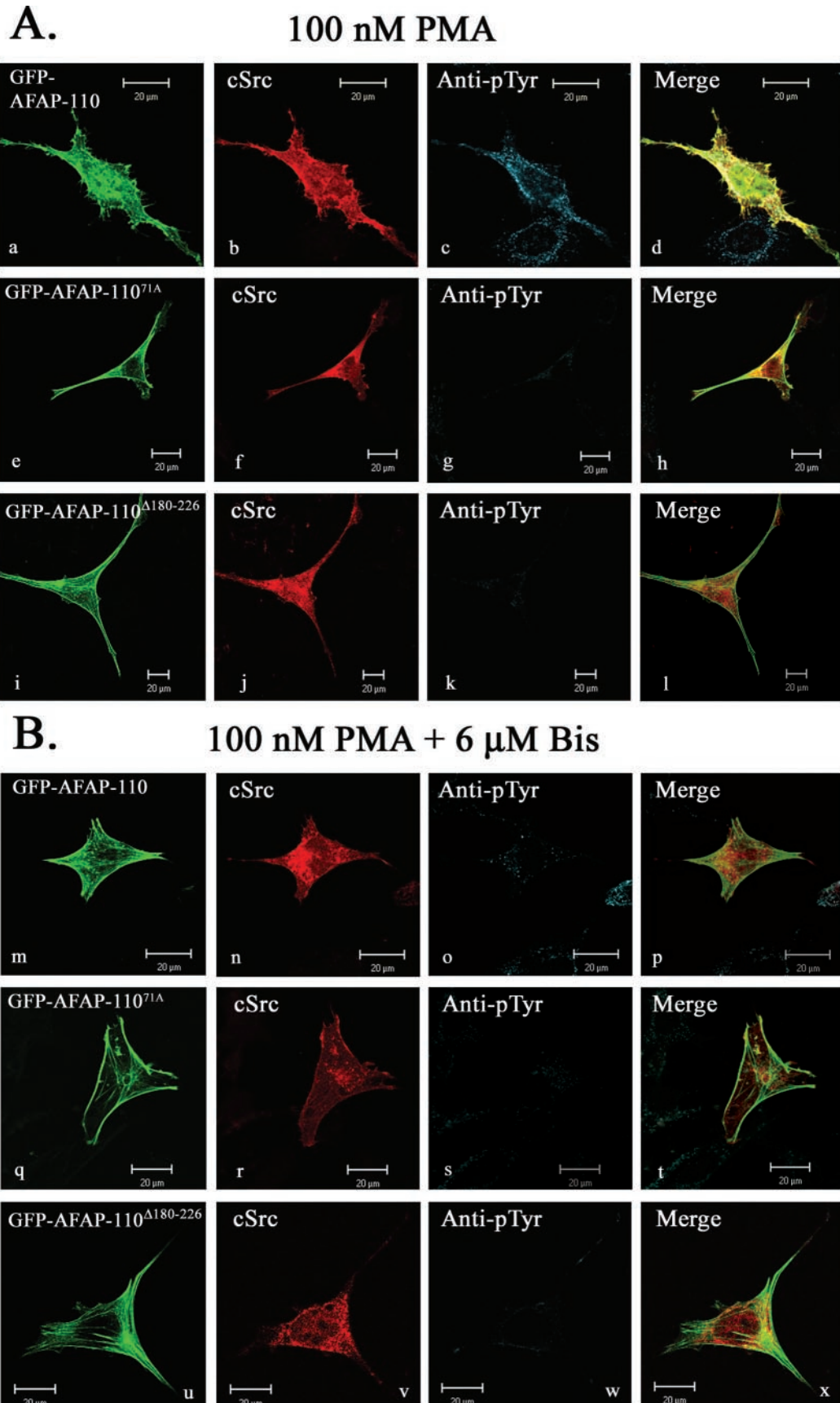


FIG. 6. PKC is present in SYF cells. SYF cells were lysed, and 40 g of protein was separated by SDS-PAGE and Western blotted with isoform-specific PKC antibodies, as indicated. Molecular weight markers are shown on the left.

PKCα activates c-Src in an AFAP-110-dependent fashion. AFAP-110 is a binding partner for both PKCα and c-Src. It was previously demonstrated that AFAP-110 is able to activate c-Src in cell culture upon removal of the autoinhibitory Lzip motif (AFAP-110^{ΔLzip}) (1, 33, 35). PKCα is able to bind to sequences in the PH1 domain of AFAP-110 that overlap with the Lzip binding motif (32, 35). Because PKCα can direct activation of c-Src and effect a conformational change in AFAP-110 that correlates with its intrinsic ability to activate c-Src, we hypothesized that AFAP-110 may be positioned to relay signals from PKCα that direct activation of c-Src. To test this hypothesis, SYF/c-Src cells were cotransfected with myrPKCα and AFAP-110. As a control, two mutant forms of AFAP-110, AFAP-110^{71A} and AFAP-110^{Δ180-226}, were also cotransfected with myrPKCα. AFAP-110^{71A} fails to bind to the c-Src SH3 domain and failed to initiate activation of c-Src (1), while AFAP-110^{Δ180-226} contains a deletion in the PH1 domain which was previously shown to prevent AFAP-110^{ΔLzip/Δ180-226} from activating c-Src (32) and to modulate localization with c-Src. The data demonstrate that myrPKCα can direct an increase in cellular tyrosine phosphorylation (Fig. 5, images a to c) and



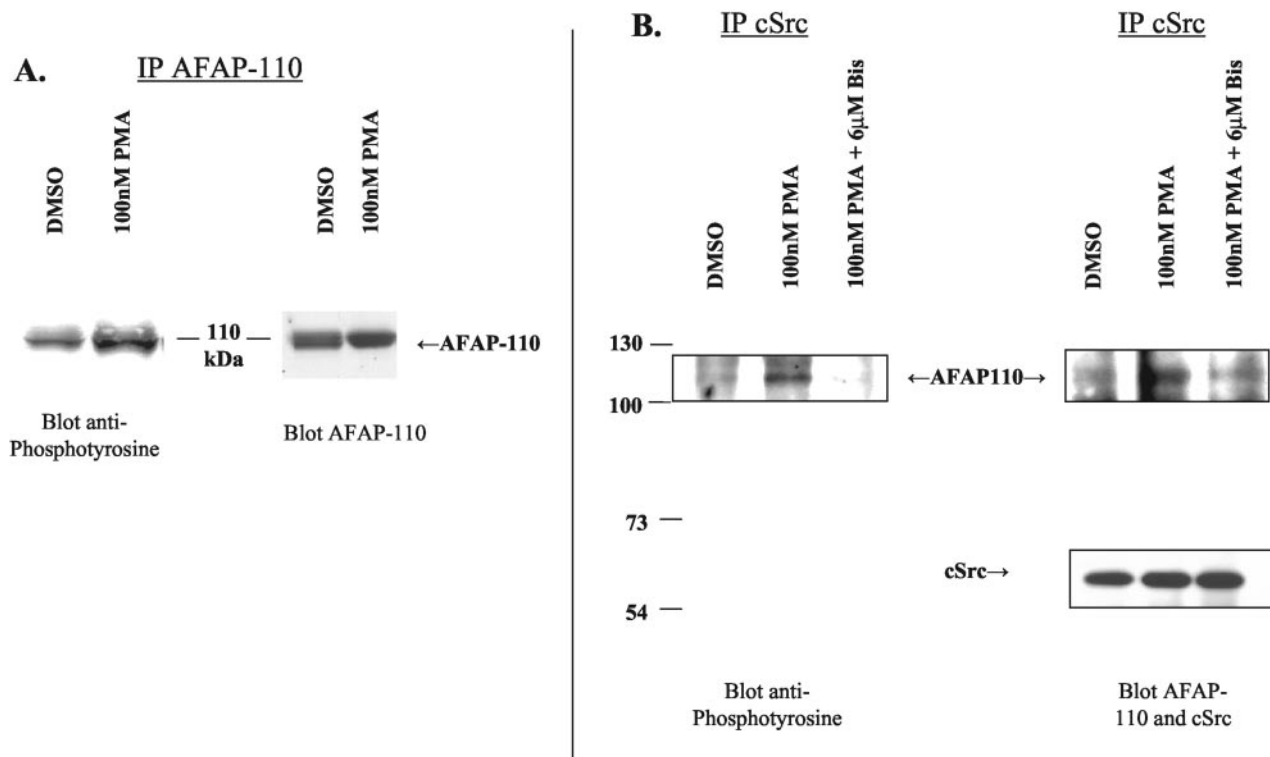


FIG. 8. PMA stimulates an increase in AFAP-110 tyrosine phosphorylation, as well as the association between AFAP-110 and c-Src in SYF/c-Src cells. (A) SYF/c-Src cells were treated with DMSO, 100 nM PMA (for 30 min), or 100 nM PMA (for 30 min) and 6 μM bisindolylmaleimide [I] (for 6 h), and AFAP-110 was immunoprecipitated (IP) from the lysates using the F1 polyclonal antibody and resolved on an SDS-8% PAGE gel. Western blot analysis was performed using an antiphosphotyrosine antibody, and the blots were stripped and reprobed for AFAP-110 with antibody F1. (B) SYF/c-Src cells were treated with DMSO, 100 nM PMA (for 30 min), or 100 nM PMA (for 30 min) and 6 μM bisindolylmaleimide [I] (Bis) (for 6 h), and c-Src was immunoprecipitated from the lysates using the anti-Src (N-18) antibody and resolved on an SDS-8% PAGE gel. Western blot analysis was performed using an antiphosphotyrosine antibody, while the blots were stripped and reprobed with antibody F1 or anti-c-Src antibodies to discern AFAP-110 levels and c-Src levels in the immunoprecipitate, respectively. AFAP-110 coimmunoprecipitated with c-Src in response to PMA treatment, while pretreatment with bisindolylmaleimide [I] resulted in abolition of this interaction.

c-Src activation (Fig. 5, images j to l). In addition, as AFAP-110 colocalizes with actin filaments (34), it is apparent that PKCα can direct AFAP-110-associated actin filaments into structures that resemble podosomes in both size and localization (Fig. 5, images a and j). However, both AFAP-110^{71A} (Fig. 5, images d to f and m to o) and AFAP-110^{Δ180-226} (Fig. 5, images g to i and p to r) blocked the ability of myrPKCα to direct actin filament reorganization. These data indicate that AFAP-110^{71A} and AFAP-110^{Δ180-226} have a dominant-nega-

tive function over PKCα in terms of activating c-Src, cellular tyrosine phosphorylation, and directing AFAP-110 to colocalize with structures that resemble podosomes. Therefore, we speculate that AFAP-110 can mediate PKCα-directed activation of c-Src and subsequent changes in actin filament organization.

To explore this further, we sought to activate endogenous PKCα with PMA and to determine whether it could direct AFAP-110 to colocalize with c-Src. PMA is a phorbol ester

FIG. 7. PMA directs AFAP-110 to colocalize with c-Src, while PKC inhibitors block PMA-induced colocalization. (A) SYF cells were transiently cotransfected with either GFP-AFAP-110 (a), GFP-AFAP-110^{71A} (e), or GFP-AFAP-110^{Δ180-226} (i) and c-Src, treated with 100 nM PMA for 30 min, and labeled with MAb EC10 (b, f, and j) and antiphosphotyrosine antibody (c, g, and k). Upon PMA stimulation, SYF cells display a loss of actin stress fiber integrity (a), as well as an increase in immunoreactivity with the antiphosphotyrosine antibody (c). PMA treatment also induced colocalization of GFP-AFAP-110 and c-Src (d). Cells cotransfected with GFP-AFAP-110^{71A} (e) and c-Src displayed immunoreactivity with the antiphosphotyrosine antibody equivalent to that of surrounding nontransfected cells (g) in response to PMA treatment. Cells cotransfected with GFP-AFAP-110^{Δ180-226} (i) and c-Src displayed immunoreactivity with the phosphotyrosine antibody equivalent to that of surrounding nontransfected cells (k) in response to PMA treatment. (B) SYF cells were cotransfected with either GFP-AFAP-110 (m), GFP-AFP-110^{71A} (q), or GFP-AFAP-110^{Δ180-226} (u) and c-Src and pretreated with 6 μM bisindolylmaleimide [I] for 6 h and 100 nM PMA for 30 min and then fixed and labeled with EC10 MAb (n, r, and v) and antiphosphotyrosine antibody (o, s, and w). In the presence of bisindolylmaleimide [I], PMA treatment of cells cotransfected with GFP-AFAP-110 and c-Src resulted in no changes in actin filament integrity (m). Likewise, bisindolylmaleimide [I] treatment blocked PMA-induced elevation in cellular tyrosine phosphorylation levels (o) and the colocalization of GFP-AFAP-110 and c-Src (p). In the presence of bisindolylmaleimide [I], PMA treatment of cells cotransfected with GFP-AFAP-110^{71A} and c-Src resulted in no elevation in cellular tyrosine phosphorylation (s). Similar results were observed in cells cotransfected with GFP-AFAP-110^{Δ180-226} and c-Src (u to x). EC10 was visualized with Cy5 anti-mouse IgG, while antiphosphotyrosine was visualized with TRITC-anti-rabbit IgG.

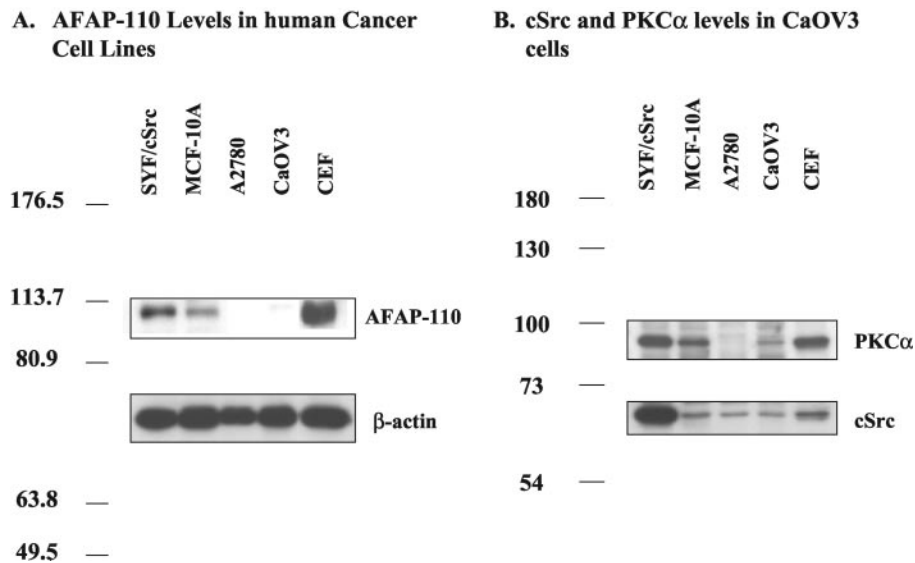


FIG. 9. AFAP-110 is not detected in CaOV3 ovarian cancer cells. Confluent monolayers of SYF/c-Src, MCF10A, A2780, CaOV3, and CEF cells were lysed, and 25 μ g of protein was separated on an SDS-8% PAGE gel. (A) Western blot analysis was performed using F1 polyclonal antibody to determine AFAP-110 levels and monoclonal antiactin antibody as a loading control. The blots were done separately, and the results were combined. (B) Western blot analysis was performed using c-Src N-16 polyclonal antibody and anti-PKC MAB to detect endogenous c-Src and PKC protein levels. The blots were done separately, and the results were combined.

that directs the activation of classical (α , β , and γ) and novel (δ , ϵ , and η) PKC family members (reference 45; reviewed in reference 2). In order to verify the expression pattern of PKC family members in SYF cells, we performed Western blot analysis of SYF cell lysates with antibodies that immunoreact with individual PKC isoforms (Fig. 6). The data demonstrate that among the PKC family members, PKC α is strongly represented, as are PKC δ and $-\lambda$ and, to a lesser extent, PKC ϵ . Previous data indicate that AFAP-110 is a substrate and binding partner for PKC α and a potential binding partner for PKC β , $-\gamma$, and $-\lambda$ as well (32). These data indicate that the PKC α isoform is the only one present in SYF cells that can (i) bind AFAP-110 and (ii) be activated by PMA. c-Src was then coexpressed with AFAP-110 in SYF cells, and the cells were treated with 100 nM PMA for 30 min to activate endogenous PKC α . Immunofluorescence analysis demonstrates that in the presence of PMA, there is a loss in actin filament organization (as evidenced by AFAP-110 localization), with podosome-like structures present, increased cellular tyrosine phosphorylation, and AFAP-110 and c-Src colocalization (Fig. 7A, images a to d). However, cells expressing mutants unable to bind c-Src (AFAP-110^{71A}) or PKC α (AFAP-110 ^{Δ 180-226}) retained normal actin filament integrity after PMA treatment and background levels of cellular tyrosine phosphorylation (Fig. 7A, images e to l), indicating that interactions with both PKC α and c-Src are required for c-Src activation and alterations in actin filament integrity. Furthermore, AFAP-110 ^{Δ 180-226} failed to colocalize with c-Src in response to PMA stimulation (Fig. 7A, image l). As a control, a 6-h pretreatment with 6 μ M bisindolylmaleimide [I] was used to block PKC α activity, resulting in AFAP-110 being unable to colocalize with c-Src in response to PMA, and it also blocked the PMA-mediated increase in cellular tyrosine phosphorylation (Fig. 7B, images m to x). These data suggest that the ability of PMA to mobilize colocalization of AFAP-

110 with c-Src is dependent upon activation of PKC α and not upon other PMA-inducible proteins (2).

To verify that PKC α activation was directing interactions between AFAP-110 and c-Src, SYF/c-Src cells were treated with dimethyl sulfoxide (DMSO) or 100 nM PMA, and the lysates were subjected to immunoprecipitation and Western blot analysis. Treatment with PMA resulted in a relative increase in endogenous AFAP-110 tyrosine phosphorylation (Fig. 8A), as well as the direct association of AFAP-110 and c-Src, as demonstrated by the ability to immunoprecipitate endogenous c-Src and to Western blot for bound endogenous AFAP-110 (Fig. 8B). Pretreatment with bisindolylmaleimide [I] resulted in an inhibition of c-Src and AFAP-110 tyrosine phosphorylation to levels equivalent to the DMSO control lane. Likewise, bisindolylmaleimide [I] treatment resulted in the abolition of binding between c-Src and AFAP-110. These data are in agreement with the immunofluorescence microscopy data and indicate that in response to PKC α activation, AFAP-110 forms a direct interaction with c-Src that correlates with increased tyrosine phosphorylation of AFAP-110.

The presence of AFAP-110 is required for PKC α -directed c-Src activation and podosome formation. Because dominant-negative AFAP-110^{71A} and AFAP-110 ^{Δ 180-226} were able to block PKC α -directed activation of c-Src, we sought to determine whether the presence of AFAP-110 was required for myrPKC α -directed activation of c-Src and subsequent podosome formation. We hypothesized that if AFAP-110 was required, then in cells that lack AFAP-110, activation of PKC α would fail to direct an increase in c-Src activation and subsequent podosome formation. We screened various human cancer cell lines for steady-state expression levels of AFAP-110 and found that in A2780 and CaOV3 cells, AFAP-110 expression levels were at or below detection limits (Fig. 9A). CaOV3 cells do express detectable levels of c-Src and PKC α , although

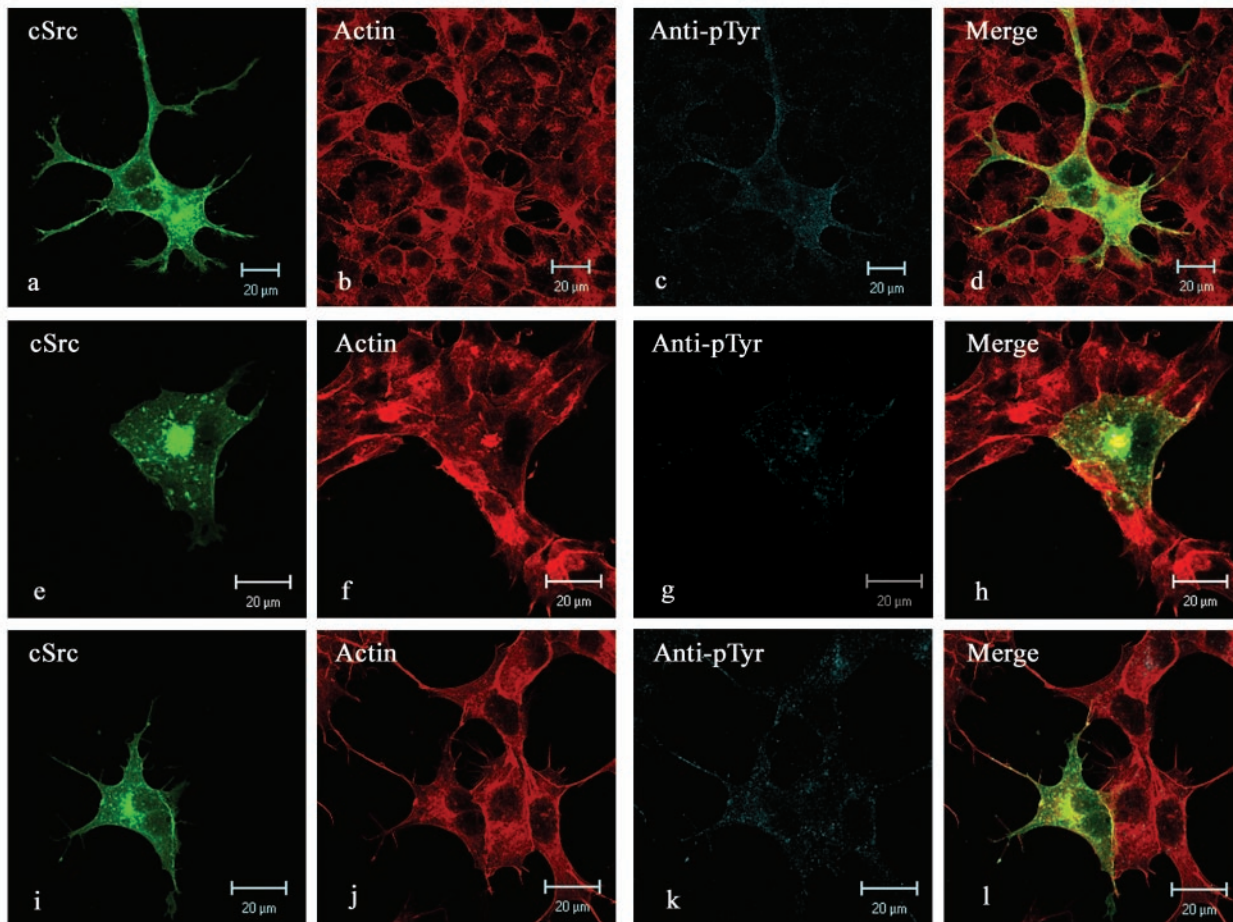
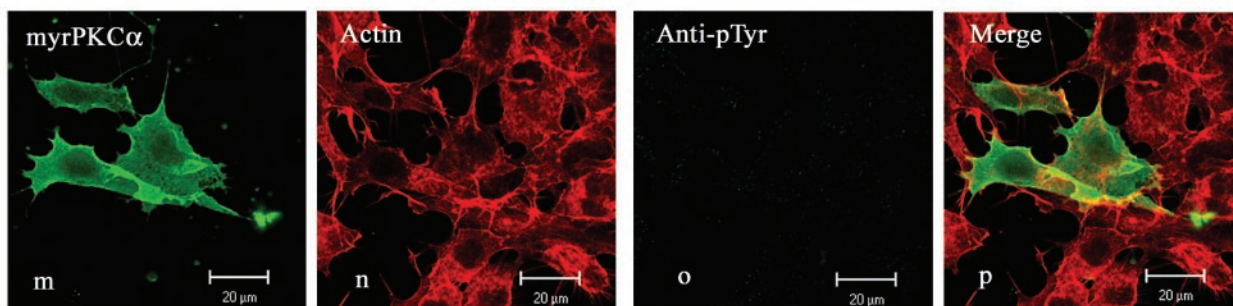
A.**B.**

FIG. 10. PMA treatment of CaOV3 cells overexpressing c-Src does not result in a significant increase in cellular tyrosine phosphorylation. (A) CaOV3 cells were transiently transfected with c-Src and then treated with DMSO, 100 nM PMA (for 30 min), or 100 nM PMA (for 30 min) and 6 μ M bisindolylmaleimide [I] (for 6 h). After fixation, the cells were labeled with MAb EC10 (a, e, and i), TRITC-phalloidin (b, f, and j), and antiphosphotyrosine antibodies (c, g, and k). DMSO treatment resulted in no change in cellular morphology or actin filament integrity (a and b), and the cells displayed only slight immunoreactivity to the antiphosphotyrosine antibody compared to surrounding nontransfected cells (c). Likewise, treatment with PMA resulted in no change in cellular morphology or actin filament integrity (e and f), as well as immunoreactivity to the antiphosphotyrosine antibody comparable to that with DMSO treatment (g). Pretreatment with bisindolylmaleimide [I] produced similar results (i, j, and k). (B) myr-PKC was transiently transfected into CaOV3 cells and labeled with anti-Flag MAb (m), TRITC-phalloidin (n), and antiphosphotyrosine antibody (o). Expression of myrPKC had no effect on cell morphology or actin filament organization (n). These cells also displayed immunoreactivity to the antiphosphotyrosine antibody equivalent to that of surrounding nontransfected cells (o). EC10 and anti-Flag MAbs were visualized with Alexa Fluor 488–goat anti-mouse IgG, and antiphosphotyrosine was visualized with Alexa Fluor 647–goat anti-rabbit IgG. Actin was visualized by staining it with TRITC-phalloidin.

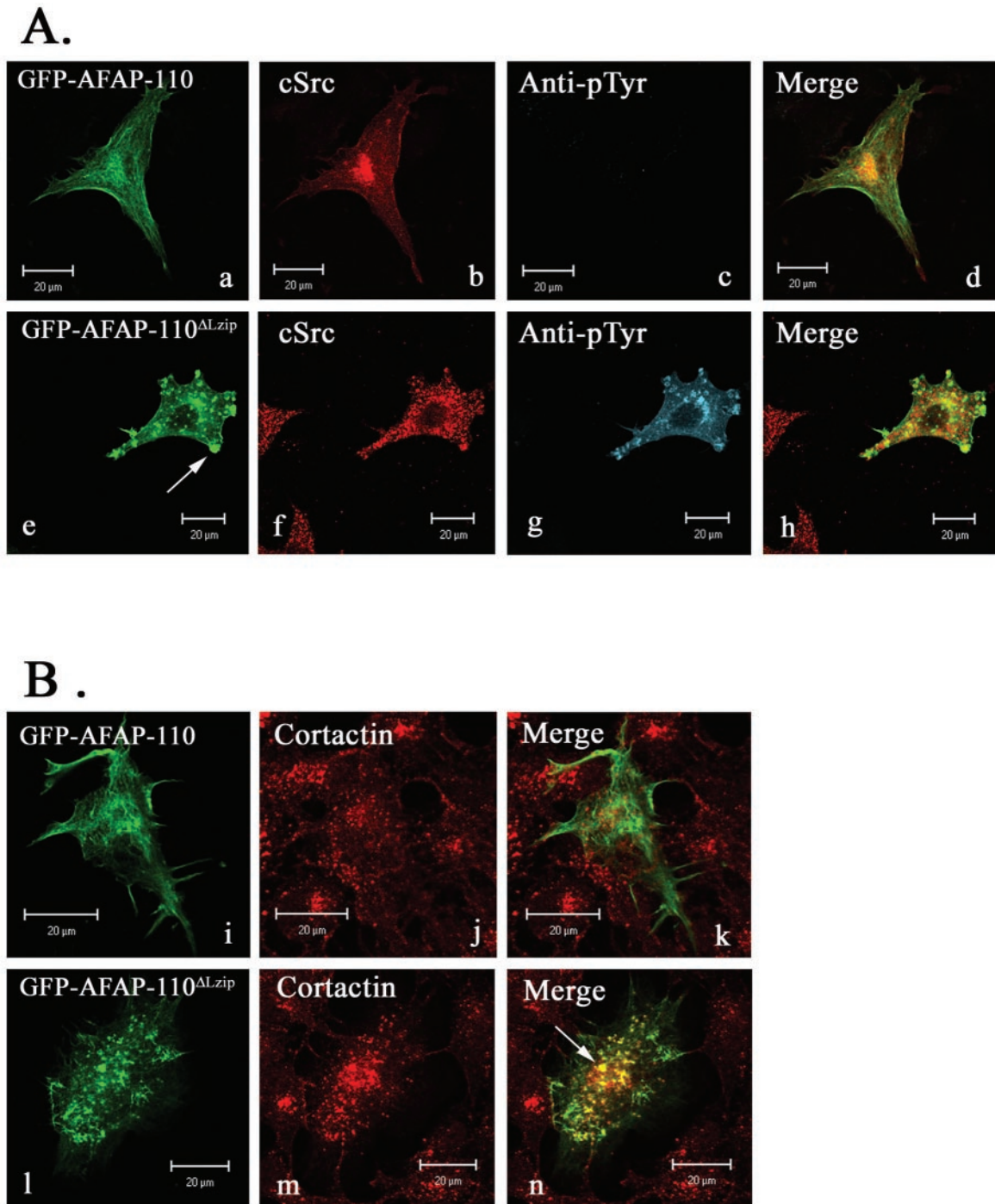


FIG. 11. AFAP-110^{ΔLzip} elevates cellular tyrosine phosphorylation and the formation of actin rosette structures in CaOV3 cells. (A) CaOV3 cells were transiently transfected with either GFP-AFAP-110 (a) or GFP-AFAP-110^{ΔLzip} (e) and c-Src (b and f) and immunolabeled with antiphosphotyrosine antibody (c and g). Expression of GFP-AFAP-110 and c-Src resulted in no significant increase in cellular tyrosine phosphorylation (c). Alternatively, expression of GFP-AFAP-110^{ΔLzip} resulted in a significant increase in cellular tyrosine phosphorylation (g), as well as the disruption of actin filament integrity and the formation of actin-rich podosome structures (e [arrow]). (B) CaOV3 cells were transiently transfected with either GFP-AFAP-110 (i) or GFP-AFAP-110^{ΔLzip} (l) and c-Src and immunolabeled with anticortactin antibody (j and m). Expression of GFP-AFAP-110 (i) does not result in the formation of podosomes, as indicated by the diffuse cortactin staining (j). Expression of GFP-AFAP-110^{ΔLzip} results in the alteration of actin stress fiber integrity and the formation of cortactin-rich podosomes (n [arrow]). EC10 was visualized with Alexa Fluor 546-goat anti-mouse IgG, anticortactin antibody was visualized with Alexa Fluor 647-goat anti-mouse IgG, and antiphosphotyrosine was visualized with Alexa Fluor 647-goat anti-rabbit IgG.

expression levels were relatively low (Fig. 9B). Thus, we chose to utilize the human ovarian cancer CaOV3 cell line to determine whether activation of PKC α required AFAP-110 to activate c-Src and effect podosome formation.

In each case where AFAP-110 constructs are able to activate c-Src, there is a concomitant increase in cellular tyrosine phosphorylation. As endogenous c-Src levels are low in CaOV3 cells, we ectopically expressed c-Src and used the MAb EC10 to visualize the localization of c-Src. However, it was first important to demonstrate that the expression of exogenous c-Src did not stimulate an increase in cellular tyrosine phosphorylation upon activation of PKC α . Treatment of CaOV3 cells expressing c-Src alone with DMSO (the solvent for PMA) did not significantly increase cellular phosphotyrosine levels relative to background (Fig. 10A, images a to d). Likewise, treatment with PMA was also unable to effect significant changes in cellular phosphotyrosine levels (Fig. 10A, images e to h). As a control, we pretreated CaOV3 cells with bisindolylmaleimide [I] to block PMA-directed PKC α signaling (Fig. 10A, images i to l). Expression of myrPKC α in CaOV3 cells was also unable to effect significant changes in cellular tyrosine phosphorylation or podosome formation (based on the appearance of F-actin) above background (Fig. 10B, images m to p). Therefore, we conclude that activation of PKC α in CaOV3 cells overexpressing exogenous c-Src does not lead to a significant increase in cellular tyrosine phosphorylation or the formation of podosomes.

In order to determine if AFAP-110 could mediate c-Src activation in CaOV3 cells, we transfected vectors expressing GFP-AFAP-110 or GFP-AFAP-110 ^{Δ Lzip} into CaOV3 cells and examined cellular tyrosine phosphorylation levels and podosome formation. In the presence of wild-type GFP-AFAP-110, no elevation in cellular tyrosine phosphorylation or podosome formation was observed (Fig. 11A, images a to d). However, expression of the dominant-positive AFAP-110 ^{Δ Lzip} construct resulted in an increase in cellular tyrosine phosphorylation, as well as the formation of AFAP-110 ^{Δ Lzip}-associated podosomes (Fig. 11A, images e to h), a phenotype similar to c-Src activation. Similarly, AFAP-110 ^{Δ Lzip} and c-Src coexpression also resulted in an increase in c-Src activation, as revealed by antiphospho (Y416) antibodies (data not shown). Immunostaining with a polyclonal cortactin antibody demonstrated that in response to AFAP-110 ^{Δ Lzip} expression, AFAP-110 ^{Δ Lzip} and cortactin colocalized in podosomes (Fig. 11B, images l to n), unlike AFAP-110 and cortactin (Fig. 11B, images i to k). These data indicate that dominant-positive AFAP-110 ^{Δ Lzip} is capable of stimulating an increase in cellular tyrosine phosphorylation and podosome formation in CaOV3 cells.

To address the issue of whether the presence of AFAP-110 could rescue the ability of PKC α to stimulate c-Src activation and podosome formation in CaOV3 cells, we ectopically expressed both AFAP-110 and c-Src in these cells using a dual expression vector to ensure successful coexpression in all transfected cells. The cells were then stimulated with DMSO, 100 nM PMA, or 100 nM PMA plus 6 μ M bisindolylmaleimide [I]. Transfected cells treated with DMSO displayed no change in cellular phosphotyrosine levels (Fig. 12A, images a to d) or colocalization of AFAP-110 and c-Src (data not shown). However, PMA treatment directed an increase in cellular tyrosine

phosphorylation and the formation of podosomes (Fig. 12A, images e to h). AFAP-110 and c-Src also colocalized in response to PMA treatment (data not shown). Pretreatment with bisindolylmaleimide [I] resulted in complete abolishment of PMA-induced effects on AFAP-110 and c-Src colocalization, cellular tyrosine phosphorylation, and podosome formation (Fig. 12A, images i to l). Likewise, PMA treatment also resulted in an increase in c-Src activation (Fig. 12B, images q to t), and this elevation in c-Src activation is abolished by pretreatment with bisindolylmaleimide [I] (Fig. 12B, images u to x). Collectively, these data indicate that AFAP-110 plays an important role in relaying signals from PKC α that direct activation of c-Src and podosome formation.

As the expression of exogenous AFAP-110 in CaOV3 cells made the cells sensitive to treatment with PMA, we next asked if mutants of AFAP-110 that were unable to either interact or colocalize with c-Src could abolish the effects we observed following treatment with PMA. CaOV3 cells transiently transfected with the Src binding mutant AFAP-110^{71A} displayed normal cell morphology and no elevation in cellular tyrosine phosphorylation in response to treatment with DMSO, and AFAP-110^{71A} and c-Src do not appear to colocalize in the merged image (Fig. 13A, images a to d). In response to treatment with 100 nM PMA, actin filament integrity was unchanged and there was no elevation in cellular tyrosine phosphorylation (Fig. 13A, images e to h); however, AFAP-110^{71A} and c-Src colocalized. This effect was abolished upon pretreatment with 6 μ M bisindolylmaleimide [I] (Fig. 13A, images i to l). In a similar manner, expression of the PKC α binding mutant AFAP-110 ^{Δ 180-226} did not alter actin filament integrity or cellular tyrosine phosphorylation in response to 100 nM PMA treatment (Fig. 13B, images m to x). However, unlike AFAP-110^{71A}, AFAP-110 ^{Δ 180-226} and c-Src were not colocalized in response to PMA treatment, indicating that AFAP-110 is capable of relaying signals from PKC α to c-Src, resulting in c-Src activation, increased cellular tyrosine phosphorylation, and the formation of podosomes.

DISCUSSION

There is significant evidence to indicate the existence of cross talk between PKC α and c-Src. Activation of each of these kinases results in substantial changes in actin filament integrity and cell morphology. Both c-Src and PKC α activation direct the formation of motility structures (lamellipodia and filopodia), and both kinases can be detected in podosomes (26). In fact, c-Src and PKC α activation is sufficient to induce the formation of podosomes (19, 26, 42). Further, both kinases will stimulate increased cell motility and invasive potential (reviewed in references 6, 14, 22, and 40). Although several studies have documented the fact that activation of c-Src results in the subsequent activation of PKC α , other studies have conversely demonstrated that PKC α can direct the activation of c-Src (3-5). The ability of PKC α to activate c-Src is not due to direct interactions between the two kinases. Although PKC α can phosphorylate c-Src, *in vitro* studies using purified c-Src and PKC α demonstrated that PKC α was unable to directly activate c-Src (4). Thus, the ability of PKC α to activate c-Src was likely due to the activity of other proteins that relayed signals from PKC α , which in turn directed the activation of

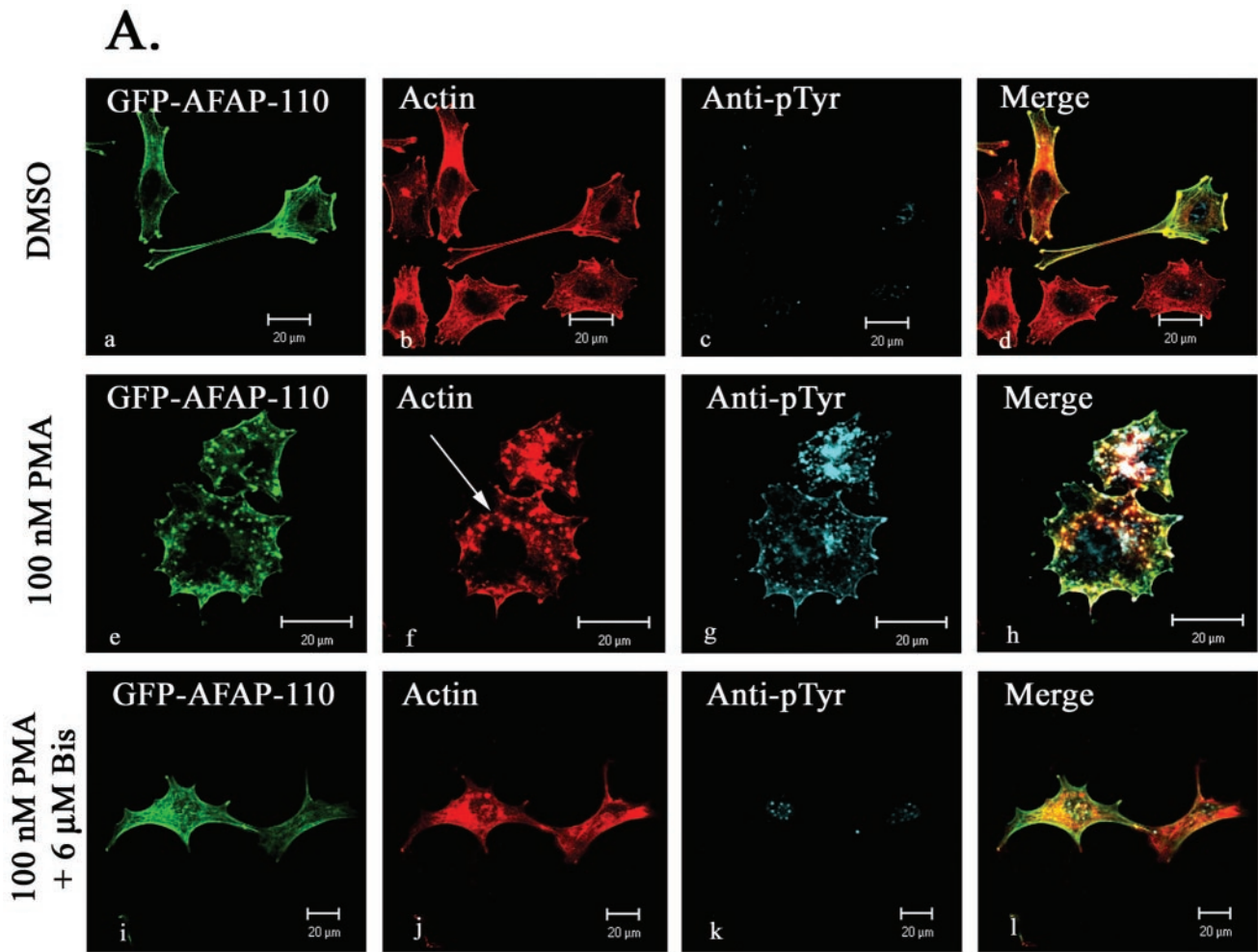


FIG. 12. Expression of AFAP-110 results in an increase in cellular tyrosine phosphorylation and c-Src activation in response to PMA treatment of CaOV3 cells. CaOV3 cells were transiently transfected with the dual expression vector pCMV-AFAP-110/c-Src and then treated with DMSO, 100 nM PMA (for 30 min), or 100 nM PMA (for 30 min) and 6 μ M bisindolylmaleimide [I] (for 6 h). After fixation, the cells were immunolabeled with the AFAP-110 MAb 4C3 (a, e, i, m, q, and u), TRITC-phalloidin (b, f, j, n, r, and v), and either antiphosphotyrosine (c, g, and k) or phospho-Src family (Y416) antibody (o, s, and w). Treatment with DMSO resulted in immunoreactivity to the antiphosphotyrosine antibody equivalent to that of surrounding nontransfected cells (c), as well as no elevation of Src kinase activity (o). DMSO treatment also had no effect on actin filament integrity (b and n). Treatment with PMA resulted in the loss of actin stress fiber integrity and the formation of actin-rich podosome structures (f and r [arrows]). Likewise, in response to PMA treatment, transfected cells displayed a great increase in immunoreactivity to the antiphosphotyrosine antibody (g) and elevated Src kinase activity (s) compared to surrounding nontransfected cells. Pretreatment with bisindolylmaleimide [I] resulted in complete abolition of the affects observed upon treatment with PMA (i to l and u to x). 4C3 MAb was visualized with Alexa Fluor 488-goat anti-mouse IgG, and actin was visualized with TRITC-phalloidin, while antiphosphotyrosine and phospho-Src family (Y416) antibodies were visualized with Alexa Fluor 647-goat anti-rabbit IgG.

c-Src. In this study, we sought to determine whether the c-Src and PKC α binding partner AFAP-110 was responsible for mediating PKC α -directed activation of c-Src and the subsequent changes in the cytoskeleton that are hallmarks of Src activation, namely, podosome formation.

Previous work demonstrated that AFAP-110 has an intrinsic ability to cross-link actin filaments and activate c-Src, and both of these functions were regulated by the Lzip motif, which provides an autoinhibitory function (1, 35). Mechanistic studies demonstrated that the Lzip motif contacted sequences in the PH1 domain that also overlapped with the PKC α binding site (32, 35). Activation of PKC α was sufficient to displace these interactions, which in turn destabilized the AFAP-110 multimer, revealing its intrinsic abilities to activate c-Src and

cross-link actin filaments (32, 33, 35). Given that (i) PKC α can activate c-Src, (ii) AFAP-110 has an intrinsic ability to activate c-Src, and (iii) PKC α can effect conformational changes in AFAP-110 that are hypothesized to release autoinhibition by the Lzip motif, we hypothesized that AFAP-110 could modulate PKC α -directed activation of c-Src and subsequent changes in the actin-based cytoskeleton that are hallmarks of c-Src activation.

Our data confirm that PKC α can direct the activation of c-Src *in vivo*. Using murine embryonic fibroblast cells, ectopic expression of constitutively activated PKC α (myrPKC α) was sufficient to direct an increase in cellular tyrosine phosphorylation and c-Src activation. An analysis of actin filament organization in these cells, using confocal microscopy and scanning

B.

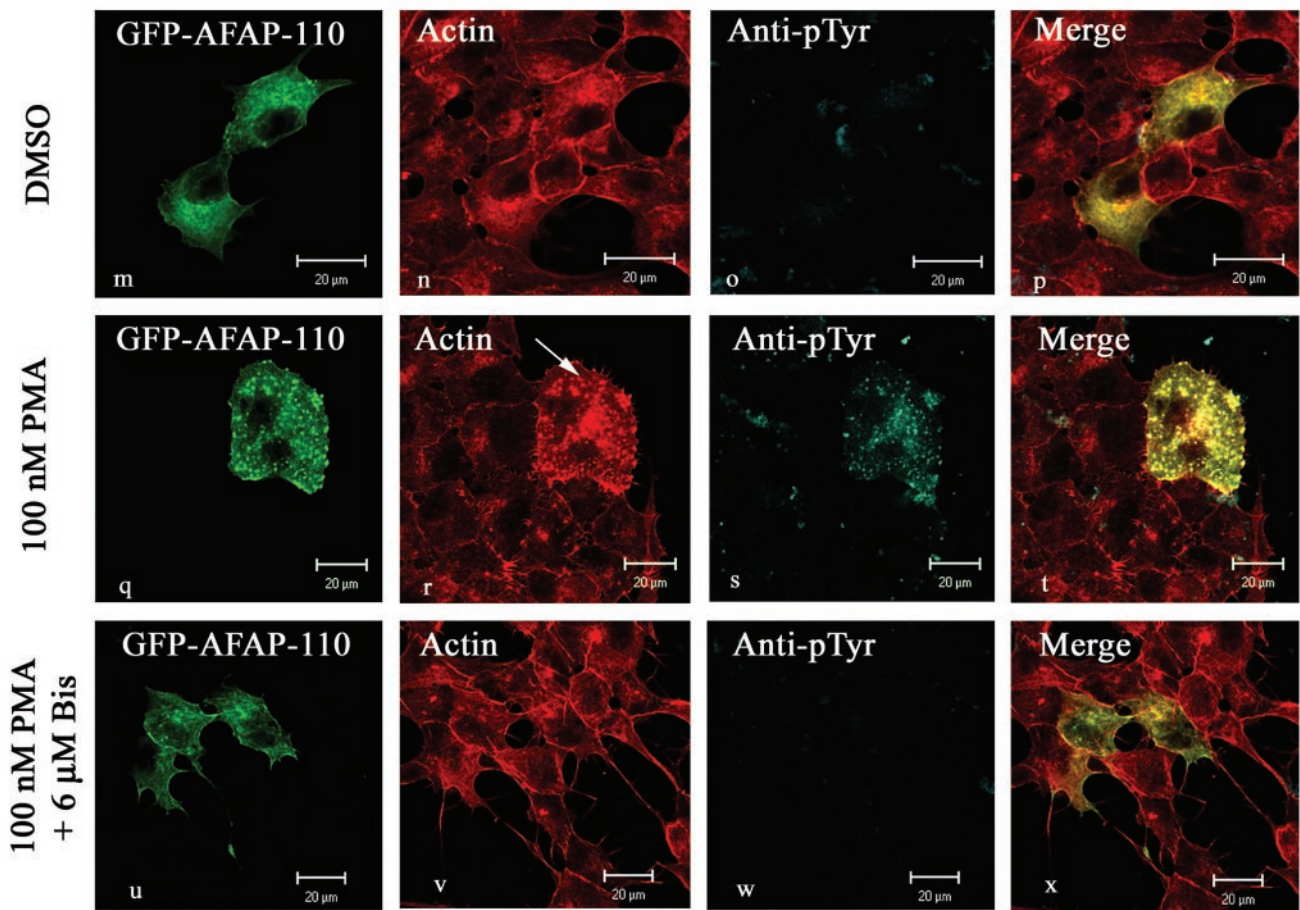


FIG. 12—Continued.

Z planes with a thickness of 1 μm , revealed the formation of actin-rich punctate structures that were ~ 0.2 to $0.5 \mu\text{m}$ in diameter and that were located on the cytoplasmic face of the ventral membrane. In addition, these structures contained cortactin. Each of these features is defining for podosomes in cells where Src is activated. The ability of PKC α to direct podosome formation and c-Src activation was dependent upon its kinase activity, as kinase-dead PKC α was unable to activate c-Src or effect podosome formation. Interestingly, the ability of activated PKC α to effect significant changes in stress filament organization and podosome formation was also dependent upon the presence of c-Src. Thus, PKC α can activate c-Src and direct podosome formation, and furthermore, PKC α requires c-Src in order to effect podosome formation and changes in stress filament integrity.

Previous work demonstrated that AFAP-110 aligns strictly with stress filaments and the cortical actin matrix (34). Deletion of the Lzip motif releases autoinhibition and enables AFAP-110 $^{\Delta\text{Lzip}}$ to activate c-Src and effect significant changes in cellular morphology. Our data demonstrate that AFAP-110 $^{\Delta\text{Lzip}}$ is able to direct an increase in cellular tyrosine phosphorylation and confirm that AFAP-110 is able to direct the activation of c-Src. The ability of AFAP-110 $^{\Delta\text{Lzip}}$ to activate

c-Src was dependent upon its ability to (i) engage the c-Src SH3 domain and (ii) colocalize with c-Src. With regard to the latter, we had previously shown that deletions in the PH1 domain, as well as point mutations which prevent SH3 binding to c-Src, were able to abolish the ability of AFAP-110 $^{\Delta\text{Lzip}}$ to activate c-Src. Here, we demonstrate that deletions in the PH1 domain prevent colocalization of AFAP-110 $^{\Delta\text{Lzip}}$ with c-Src and the subsequent activation of c-Src. In vitro kinase data support this hypothesis, as both recombinant AFAP-110 and recombinant AFAP-110 $^{\Delta\text{Lzip}}$ have the potential to activate c-Src, but in cells, only AFAP-110 $^{\Delta\text{Lzip}}$ can direct c-Src activation. These data indicate that (i) AFAP-110 is capable of activating c-Src and (ii) upon release of the Lzip motif from the PH1 domain, AFAP-110 is directed to move to and colocalize with c-Src in a fashion dependent upon the integrity of the PH1 domain. Although we do not know how the PH1 domain facilitates colocalization, it is well known that pleckstrin homology domains can function as both protein and lipid binding partners (reviewed in reference 25). Thus, it is possible that a protein chaperone delivers AFAP-110 to c-Src or, conversely, that lipid and/or membrane binding properties are revealed that promote colocalization with c-Src. This mechanism is under investigation. Interestingly, the ability of AFAP-110 $^{\Delta\text{Lzip}}$ to

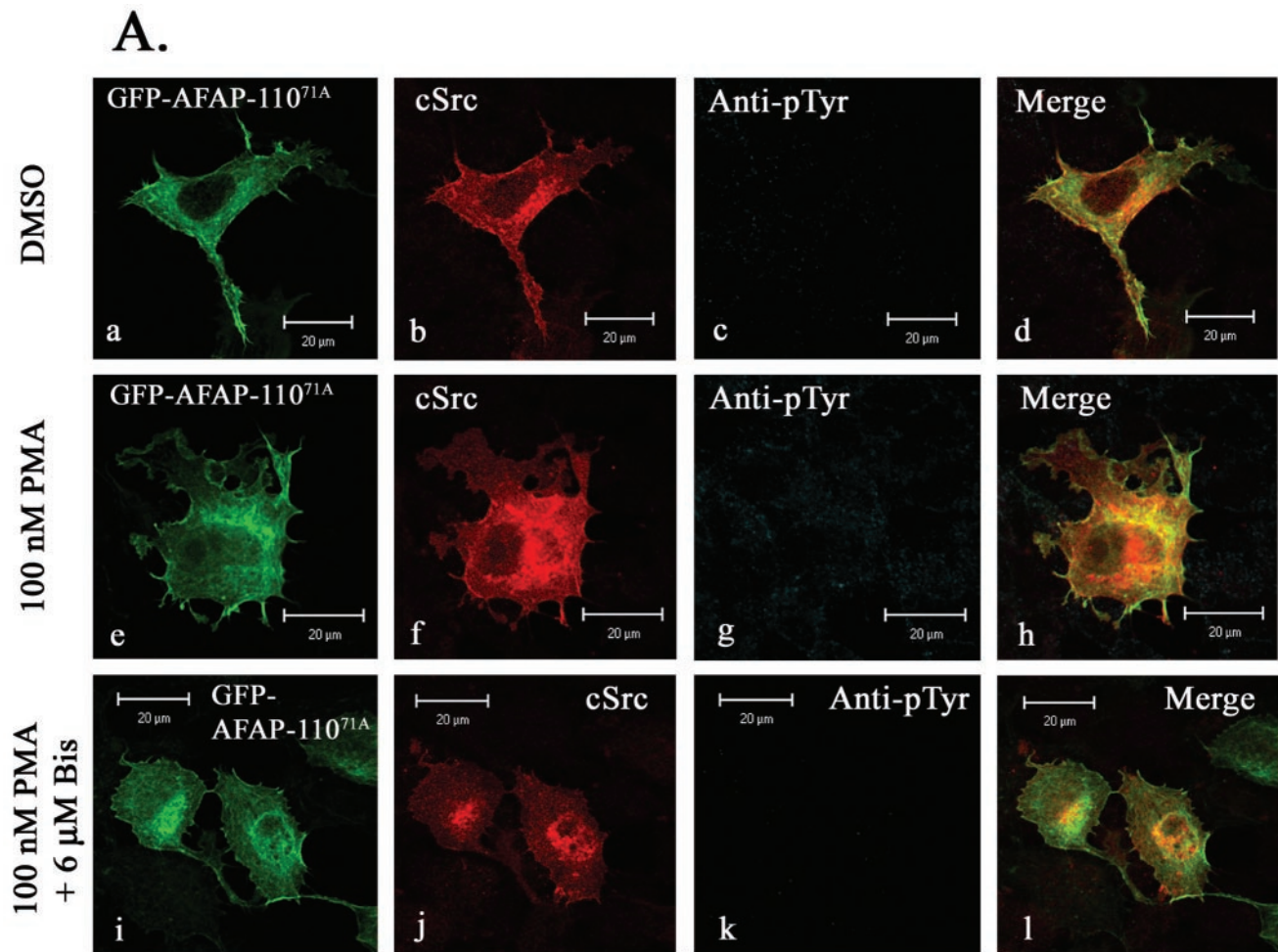


FIG. 13. Mutants of AFAP-110 that abolish interactions with c-Src or PKC are able to block the effects of AFAP-110 in response to PMA treatment in CAOV3 cells. (A) CAOV3 cells were transiently cotransfected with GFP-AFAP-110^{71A} (a, e, and i) and c-Src and then treated with DMSO, 100 nM PMA (for 30 min), or 100 nM PMA (for 30 min) and 6 μ M bisindolylmaleimide [I] (for 6 h). After fixation, the cells were immunolabeled with EC10 (b, f, and j) and antiphosphotyrosine antibodies (c, g, and k). PMA treatment resulted in normal cell morphology (a, e and i), as well as no change in cellular tyrosine phosphorylation (g) from that observed upon treatment with DMSO (c). Likewise, pretreatment with bisindolylmaleimide [I] and PMA also resulted in no elevation in cellular tyrosine phosphorylation above background (k). Identical results were obtained upon expression of GFP-AFAP-110 ^{Δ 180-226} and c-Src after treatment with PMA. EC10 was visualized with Alexa Fluor 546-goat anti-mouse IgG, while antiphosphotyrosine antibody was visualized with Alexa Fluor 647-goat anti-rabbit IgG. (B) Same as panel A, except that the dominant-negative mutant, AFAP-110 ^{Δ 180-226} was transfected.

direct the formation of, and colocalize with, podosomes is confirmed based on the colocalization of AFAP-110 ^{Δ Lzip} and cortactin to these actin-rich punctuate structures on the cytoplasmic face of the ventral membrane. Furthermore, the ability of AFAP-110 ^{Δ Lzip} to direct the formation of podosomes is dependent upon the presence of c-Src.

We were able to demonstrate that AFAP-110 does modulate PKC α -directed activation of c-Src by using two different techniques. Overexpression of myrPKC α in murine embryonic fibroblasts was sufficient to induce increases in cellular phosphotyrosine content and c-Src activation. Using confocal microscopy and examining scanning Z planes 1 μ m thick indicated that all of the phosphotyrosine signal and c-Src activation is detected on the cytoplasmic face of the dorsal membrane. This observation is distinct from an examination of Src^{S27F} expression in cells, where phosphotyrosine signals can be detected throughout the cell (A. Gatesman and D. C. Flynn,

unpublished observation), indicating that PKC α may direct the activation of c-Src and subsequent tyrosine phosphorylation of a subset of potential substrates. Overexpression of mutants of AFAP-110 that fail to bind the c-Src SH3 domain, or fail to colocalize with c-Src, each blocked myrPKC α from activating c-Src and directing podosome formation. Given that AFAP-110 does colocalize with cortactin in podosomes and AFAP-110 always colocalizes with F-actin, podosome formation was hypothesized based on the presence of AFAP-110 in these punctate structures along the dorsal membrane. These observations were confirmed by using PMA, an activator of endogenous PKC α . Treatment of cells with PMA resulted in activation of c-Src in an AFAP-110-dependent manner. The ability of PMA to induce the activation of c-Src was sensitive to the presence of bisindolylmaleimide [I], an inhibitor of PKC that binds to the catalytic domain. These data confirm that PMA-directed activation of c-Src occurs in a fashion dependent upon

B.

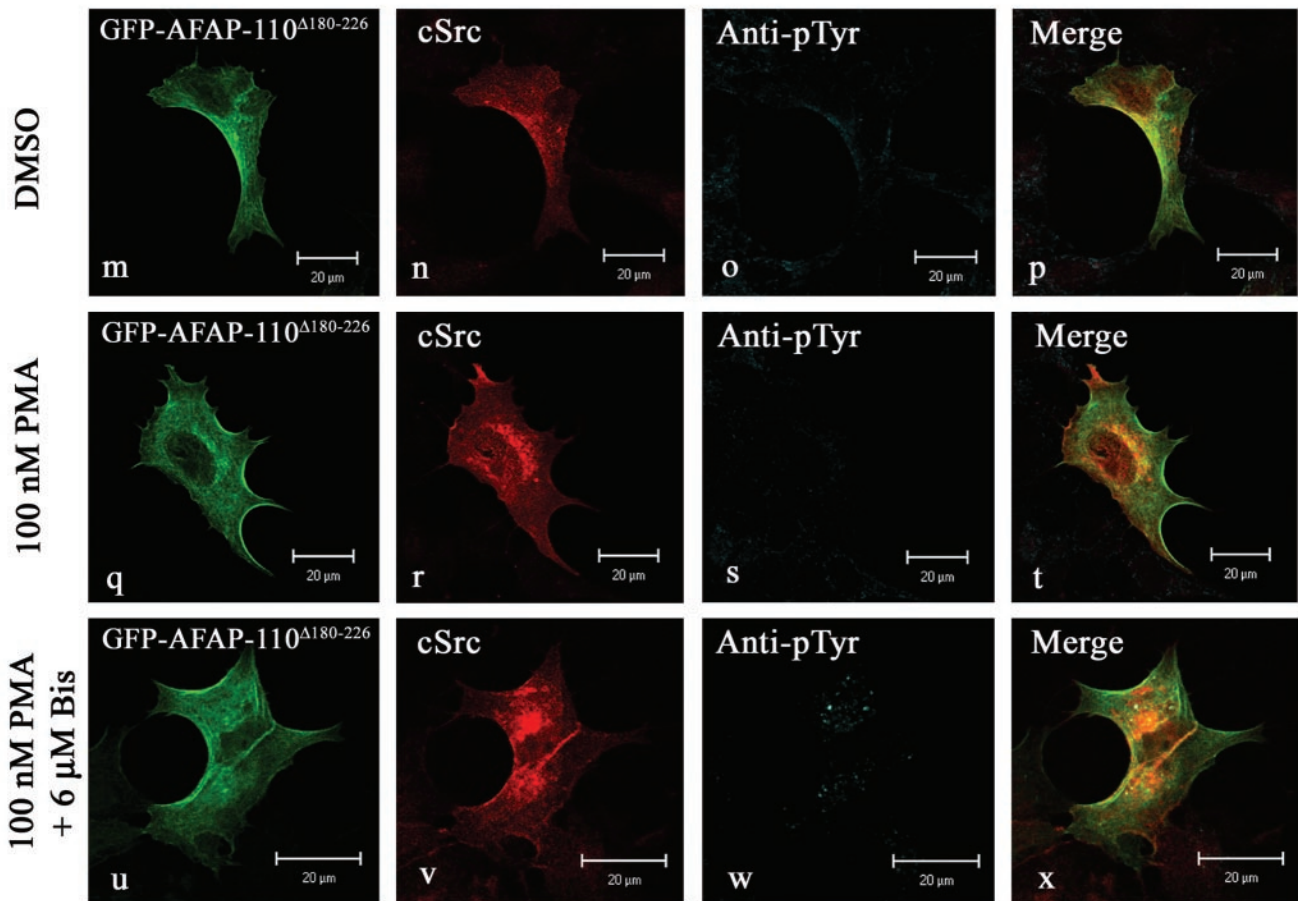


FIG. 13—Continued.

the catalytic activity of PKC and not upon any other PMA-associated functions. In addition, PMA was able to direct an increase in tyrosine phosphorylation of endogenous AFAP-110 and was able to direct complex formation between AFAP-110 and c-Src. Collectively, these data indicate that PKC α directs c-Src activation in an AFAP-110-dependent manner.

We sought to determine if PKC α could direct the activation of c-Src and podosome formation in the absence of AFAP-110. For this analysis, we utilized a cell line, CaOV3, that contained AFAP-110 protein expression levels that were at or below the levels of detection. The data indicate that neither myrPKC α nor PMA was able to induce an increase in cellular phosphotyrosine content, c-Src activation, or podosome formation. Ectopic expression of AFAP-110 Δ L^{zip} was able to direct an increase in cellular phosphotyrosine content, c-Src activation, and podosome formation, indicating that it is possible to activate these signals in these cells. Ectopic expression of AFAP-110 restored the ability of myrPKC α and PMA to stimulate the activation of c-Src, increased cellular phosphotyrosine content, and podosome formation, while mutants of AFAP-110 that fail to activate c-Src failed to relay these signals. These data confirm that AFAP-110 plays an important role in relaying signals from PKC α that direct the activation of c-Src and podosome formation.

Collectively, these data indicate that PKC α directs the activation of c-Src via AFAP-110. We hypothesize the following model. Activation of PKC α displaces autoinhibitory interactions between the Lzip motif and the PH1 domain of AFAP-110. This enables AFAP-110 to move to and colocalize with c-Src in a PH1 domain-dependent manner. AFAP-110 then initiates the activation of c-Src through SH3 binding. Activated c-Src then stimulates signals that direct the formation of podosomes. These data are significant for several reasons. First, they establish a mechanism by which PKC α can activate c-Src. Second, they establish a mechanism by which PKC α can direct the formation of podosomes. Podosomes are actin-rich structures that form on the ventral membrane and are hypothesized to play an important role in modulating the invasive potential of a cell. Both PKC α and c-Src activation are sufficient to induce an increase in cell motility and invasive potential. Indeed, it has been hypothesized that activation of c-Src occurs concomitant with acquisition of the invasive phenotype (13). Podosomes are rich in cross-linked F-actin and contain a variety of actin-binding proteins and signaling proteins, such as actin, cortactin, AFAP-110, and c-Src (26). Interestingly, AFAP-110 may contribute to the formation of podosomes in two ways. Here, PKC α would affect a conformation change upon AFAP-110 that allows it to colocalize with and activate

c-Src, which our data indicate is sufficient to initiate signals that direct podosome formation. In addition, the conformational change directed in AFAP-110 that allows it to activate c-Src is also sufficient to increase the ability of AFAP-110 to cross-link F-actin (35). Cross-linked F-actin exists in the core of the podosome. Although our analysis does not distinguish the localization of AFAP-110 in the core or fringe of a podosome, it is possible that AFAP-110 may be positioned to facilitate actin cross-linking within the newly formed podosome core. It is also possible that AFAP-110 colocalization to podosomes may be required to facilitate c-Src colocalization to podosomes, as AFAP-110 is a binding partner for activated Src (18).

These data also have implications for signal transduction and possibly cancer progression. AFAP-110 is a PH1 domain binding partner for PKC β , PKC γ , and PKC λ (32). Furthermore, AFAP-110 is an SH3 binding partner for Fyn and Lyn, but not c-Yes (12, 17, 41). Thus, AFAP-110 may be positioned to relay signals from other PKC family members that direct the activation of a subset of Src family kinases. In each instance, this may result in the formation of podosomes. Given that PKC α and c-Src expression levels and activation states are increased in a variety of invasive human cancers, it may be possible that AFAP-110 expression levels in these same cancers could facilitate the relay of signals that direct the activation of c-Src and the acquisition of the invasive phenotype. These studies are under way.

ACKNOWLEDGMENTS

We gratefully acknowledge Anne Guappone-Koay for technical assistance and Henry Zot for helpful suggestions in the preparation of the manuscript.

This work was supported by a grant to D.C.F. from the NCI (CA60731) and a grant from the NCRN CoBRE program (RR16440). A.G. was supported by an NIH training grant (T32-ES10953). V.G.W. was supported by a fellowship from the W. E. B. DuBois Foundation. J.M.B. was supported by a fellowship from the West Virginia University Medical Scientist Training Program.

REFERENCES

- Baisden, J. M., A. S. Gatesman, L. Cherezova, B. H. Jiang, and D. C. Flynn. 2001. The intrinsic ability of AFAP-110 to alter actin filament integrity is linked with its ability to also activate cellular tyrosine kinases. *Oncogene* **20**:6607–6616.
- Barry, O. P., and M. G. Kazanietz. 2001. Protein kinase C isozymes, novel phorbol ester receptors and cancer chemotherapy. *Curr. Pharm. Des.* **7**:1725–1744.
- Brandt, D., M. Gimona, M. Hillmann, H. Haller, and H. Mischak. 2002. Protein kinase C induces actin reorganization via a Src- and Rho-dependent pathway. *J. Biol. Chem.* **277**:20903–20910.
- Brandt, D. T., A. Goerke, M. Heuer, M. Gimona, M. Leitges, E. Kremmer, R. Lammers, H. Haller, and H. Mischak. 2003. Protein kinase C delta induces Src kinase activity via activation of the protein tyrosine phosphatase PTP alpha. *J. Biol. Chem.* **278**:34073–34078.
- Bruce-Staskal, P. J., and A. H. Bouton. 2001. PKC-dependent activation of FAK and src induces tyrosine phosphorylation of Cas and formation of Cas-Crk complexes. *Exp. Cell Res.* **264**:296–306.
- Carter, C. A. 2000. Protein kinase C as a drug target: implications for drug or diet prevention and treatment of cancer. *Curr. Drug Targets* **1**:163–183.
- Cramer, L. P. 1997. Molecular mechanism of actin-dependent retrograde flow in lamellipodia of motile cells. *Front. Biosci.* **2**:d260–d270.
- Delage, S., E. Chastre, S. Empereur, D. Wicek, D. Veissiere, J. Capeau, C. Gespach, and G. Cherqui. 1993. Increased protein kinase C alpha expression in human colonic Caco-2 cells after insertion of human Ha-ras or polyoma virus middle T oncogenes. *Cancer Res.* **53**:2762–2770.
- Dwyer-Nield, L. D., A. C. Miller, B. W. Neighbors, D. Dinsdale, and A. M. Malkinson. 1996. Cytoskeletal architecture in mouse lung epithelial cells is regulated by protein-kinase C-alpha and calpain II. *Am. J. Physiol.* **270**:L526–L534.
- Felice, G. R., P. Eason, M. V. Nermut, and S. Kellie. 1990. pp60v-src association with the cytoskeleton induces actin reorganization without affecting polymerization status. *Eur. J. Cell Biol.* **52**:47–59.
- Fincham, V. J., A. Chudleigh, and M. C. Frame. 1999. Regulation of p190 Rho-GAP by v-Src is linked to cytoskeletal disruption during transformation. *J. Cell Sci.* **112**:947–956.
- Flynn, D. C., T. H. Leu, A. B. Reynolds, and J. T. Parsons. 1993. Identification and sequence analysis of cDNAs encoding a 110-kilodalton actin filament-associated pp60src substrate. *Mol. Cell. Biol.* **13**:7892–7900.
- Frame, M. C. 2002. Src in cancer: deregulation and consequences for cell behaviour. *Biochim. Biophys. Acta* **1602**:114–130.
- Gomez, D. E., G. Skilton, D. F. Alonso, and M. G. Kazanietz. 1999. The role of protein kinase C and novel phorbol ester receptors in tumor cell invasion and metastasis. *Oncol. Rep.* **6**:1363–1370.
- Gould, K. L., J. R. Woodgett, J. A. Cooper, J. E. Buss, D. Shalloway, and T. Hunter. 1985. Protein kinase C phosphorylates pp60src at a novel site. *Cell* **42**:849–857.
- Gray, A., K. J. Van Der, and C. P. Downes. 1999. The pleckstrin homology domains of protein kinase B and GRP1 (general receptor for phosphoinositides-1) are sensitive and selective probes for the cellular detection of phosphatidylinositol 3,4-bisphosphate and/or phosphatidylinositol 3,4,5-trisphosphate in vivo. *Biochem. J.* **344**:929–936.
- Guappone, A. C., and D. C. Flynn. 1997. The integrity of the SH3 binding motif of AFAP-110 is required to facilitate tyrosine phosphorylation by, and stable complex formation with, Src. *Mol. Cell. Biochem.* **175**:243–252.
- Guappone, A. C., T. Weimer, and D. C. Flynn. 1998. Formation of a stable src-AFAP-110 complex through either an amino-terminal or a carboxy-terminal SH2-binding motif. *Mol. Carcinog.* **22**:110–119.
- Hai, C. M., P. Hahne, E. O. Harrington, and M. Gimona. 2002. Conventional protein kinase C mediates phorbol-dibutyrate-induced cytoskeletal remodeling in a7r5 smooth muscle cells. *Exp. Cell Res.* **280**:64–74.
- Harrington, E. O., J. Löffler, P. R. Nelson, K. C. Kent, M. Simons, and J. A. Ware. 1997. Enhancement of migration by protein kinase C α and inhibition of proliferation and cell cycle progression by protein kinase C δ in capillary endothelial cells. *J. Biol. Chem.* **272**:7390–7397.
- Imamura, H., K. Takaishi, K. Nakano, A. Kodama, H. Oishi, H. Shiozaki, M. Monden, T. Sasaki, and Y. Takai. 1998. Rho and Rab small G proteins coordinately reorganize stress fibers and focal adhesions in MDCK cells. *Mol. Biol. Cell* **9**:2561–2575.
- Irby, R. B., and T. J. Yeatman. 2000. Role of Src expression and activation in human cancer. *Oncogene* **19**:5636–5642.
- Jaken, S., K. Leach, and T. Klauck. 1989. Association of type 3 protein kinase C with focal contacts in rat embryo fibroblasts. *J. Cell Biol.* **109**:697–704.
- Klinghoffer, R. A., C. Sachsenmaier, J. A. Cooper, and P. Soriano. 1999. Src family kinases are required for integrin but not PDGFR signal transduction. *EMBO J.* **18**:2459–2471.
- Lemmon, M. A., and K. M. Ferguson. 2000. Signal-dependent membrane targeting by pleckstrin homology (PH) domains. *Biochem. J.* **350**:1–18.
- Linder, S., and M. Aepfelbacher. 2003. Podosomes: adhesion hot-spots of invasive cells. *Trends Cell Biol.* **13**:376–385.
- Lodyga, M., X. H. Bai, E. Mourgeon, B. Han, S. Keshavjee, and M. Liu. 2002. Molecular cloning of actin filament-associated protein: a putative adaptor in stretch-induced Src activation. *Am. J. Physiol. Lung Cell Mol. Physiol.* **283**:L265–L274.
- Mizutani, K., H. Miki, H. He, H. Maruta, and T. Takenawa. 2002. Essential role of neural Wiskott-Aldrich syndrome protein in podosome formation and degradation of extracellular matrix in src-transformed fibroblasts. *Cancer Res.* **62**:669–674.
- Moyers, J. S., A. H. Bouton, and S. J. Parsons. 1993. The sites of phosphorylation by protein kinase C and an intact SH2 domain are required for the enhanced response to beta-adrenergic agonists in cells overexpressing c-src. *Mol. Cell. Biol.* **13**:2391–2400.
- Provenzano, C., R. Gallo, R. Carbone, P. P. Di Fiore, G. Falcone, L. Castellani, and S. Alema. 1998. Eps8, a tyrosine kinase substrate, is recruited to the cell cortex and dynamic F-actin upon cytoskeleton remodeling. *Exp. Cell Res.* **242**:186–200.
- Purchio, A. F., M. Shoyab, and L. E. Gentry. 1985. Site-specific increased phosphorylation of pp60v-src after treatment of RSV-transformed cells with a tumor promoter. *Science* **229**:1393–1395.
- Qian, Y., J. M. Baisden, L. Cherezova, J. M. Summy, A. Guappone-Koay, X. Shi, T. Mast, J. Pustula, H. G. Zot, N. Mazloum, M. Y. Lee, and D. C. Flynn. 2002. PC phosphorylation increases the ability of AFAP-110 to cross-link actin filaments. *Mol. Biol. Cell* **13**:2311–2322.
- Qian, Y., J. M. Baisden, E. H. Westin, A. C. Guappone, T. C. Koay, and D. C. Flynn. 1998. Src can regulate carboxy terminal interactions with AFAP-110, which influence self-association, cell localization and actin filament integrity. *Oncogene* **16**:2185–2195.
- Qian, Y., J. M. Baisden, H. G. Zot, W. B. Van Winkle, and D. C. Flynn. 2000. The carboxy terminus of AFAP-110 modulates direct interactions with actin filaments and regulates its ability to alter actin filament integrity and induce lamellipodia formation. *Exp. Cell Res.* **255**:102–113.
- Qian, Y., A. S. Gatesman, J. M. Baisden, H. G. Zot, L. Cherezova, I. Qazi, N.

- Mazloun, M. Y. Lee, A. Guappone-Koay, and D. C. Flynn. 2004. Analysis of the role of the leucine zipper motif in regulating the ability of AFAP-110 to alter actin filament integrity. *J. Cell Biochem.* **91**:602–620.
36. Qian, Y., A. C. Guappone, J. M. Baisden, M. W. Hill, J. M. Summy, and D. C. Flynn. 1999. Monoclonal antibodies directed against AFAP-110 recognize species-specific and conserved epitopes. *Hybridoma* **18**:167–175.
37. Qureshi, S. A., C. K. Joseph, M. Rim, A. Maroney, and D. A. Foster. 1991. v-Src activates both protein kinase C-dependent and independent signaling pathways in murine fibroblasts. *Oncogene* **6**:995–999.
38. Redmond, T., B. K. Brott, R. Jove, and M. J. Welsh. 1992. Localization of the viral and cellular Src kinases to perinuclear vesicles in fibroblasts. *Cell Growth Differ.* **3**:567–576.
39. Reynolds, A. B., D. J. Roesel, S. B. Kanner, and J. T. Parsons. 1989. Transformation-specific tyrosine phosphorylation of a novel cellular protein in chicken cells expressing oncogenic variants of the avian cellular *src* gene. *Mol. Cell. Biol.* **9**:629–638.
40. Summy, J. M., and G. E. Gallick. 2003. Src family kinases in tumor progression and metastasis. *Cancer Metastasis Rev.* **22**:337–358.
41. Summy, J. M., A. C. Guappone, M. Sudol, and D. C. Flynn. 2000. The SH3 and SH2 domains are capable of directing specificity in protein interactions between the non-receptor tyrosine kinases cSrc and cYes. *Oncogene* **19**:155–160.
42. Tarone, G., D. Cirillo, F. G. Giancotti, P. M. Comoglio, and P. C. Marchisio. 1985. Rous sarcoma virus-transformed fibroblasts adhere primarily at discrete protrusions of the ventral membrane called podosomes. *Exp. Cell Res.* **159**:141–157.
43. Xian, W., M. P. Rosenberg, and J. DiGiovanni. 1997. Activation of erbB2 and c-src in phorbol ester-treated mouse epidermis: possible role in mouse skin tumor promotion. *Oncogene* **14**:1435–1444.
44. Zang, Q., P. Frankel, and D. A. Foster. 1995. Selective activation of protein kinase C isoforms by v-Src. *Cell Growth Differ.* **6**:1367–1373.
45. Zhou, L. Y., M. Disatnik, G. S. Herron, D. Mochly-Rosen, and M. A. Karasek. 1996. Differential activation of protein kinase C isozymes by phorbol ester and collagen in human skin microvascular endothelial cells. *J. Investig. Dermatol.* **107**:248–252.